BILINGUAL PUBLISHING CO.
Pioneer of Global Academics Since 1984

Organic Polymer Material Research

Volume 3 | Issue 1 | June 2021 | ISSN 2661-3875（Online）

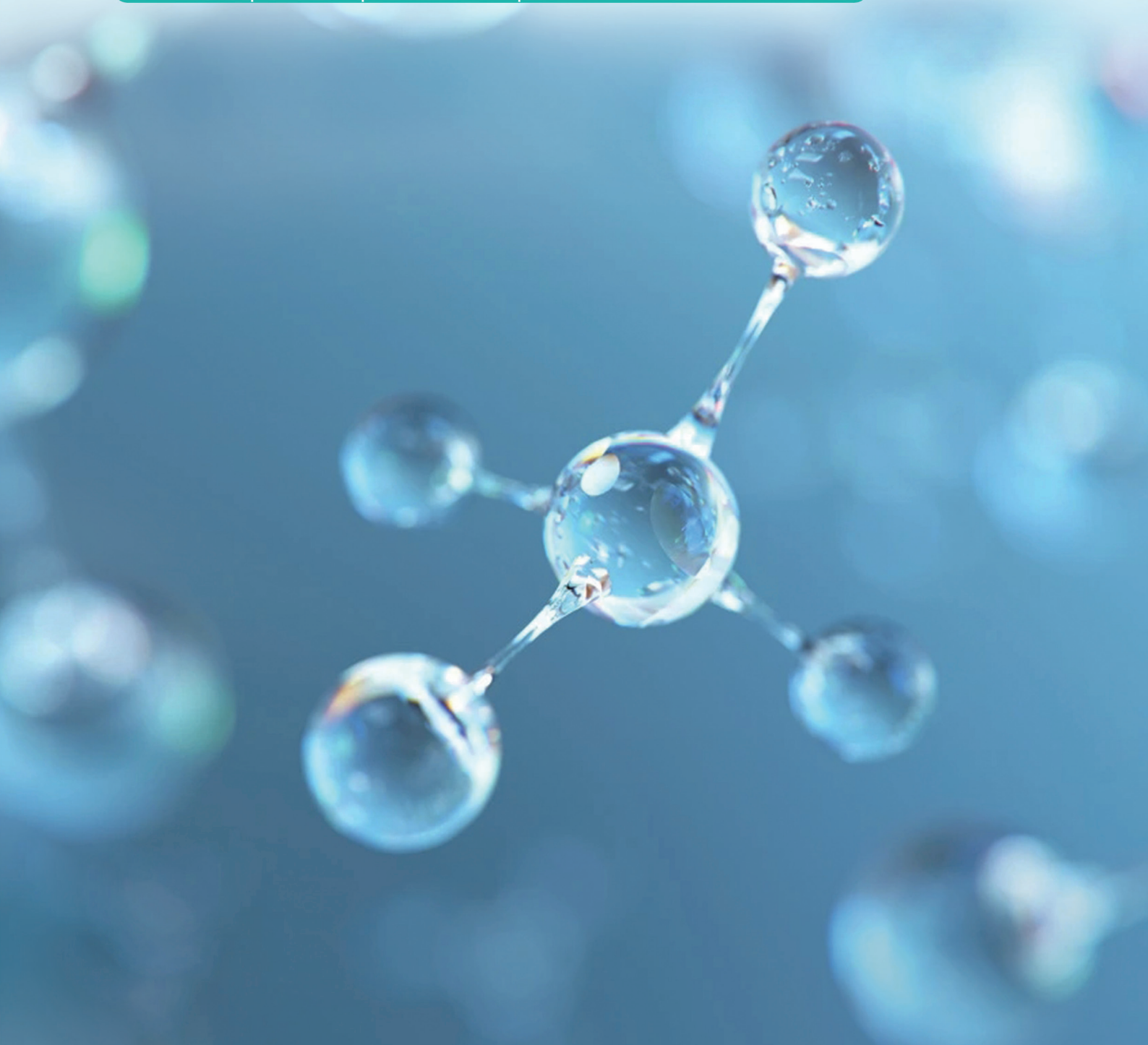

Volume 3 Issue 1 • June 2021 • ISSN 2661-3875 (Online)

Organic Polymer Material Research

Editor-in-Chief

Dr. Yanmin Wang

BILINGUAL PUBLISHING CO.
Pioneer of Global Academics Since 1984

BILINGUAL PUBLISHING CO.
Pioneer of Global Academics Since 1984

Volume 3 | Issue 1 | June 2021 | Page1-31
Organic Polymer Material Research

Contents

Articles

1 **AC Impedance and FTIR Studies of PVA-$ZnCl_2$ Based Solid Polymer Electrolytes**

Jayanthi S

5 **Development of NR/SBR Based Rubber Compounds with Low Hysteresis and High Durability for Transmission V-Belts Applications**

Asit Baran Bhattacharya M. Pandy Kinsuk Naskar

17 **Impact of Mixed Fillers on the Physico-mechanical Properties of Flexible Polyether Foam**

Onwuka, C.O. Anekwe, O. J. Ogudo, M.C. Chris-Okafor, P.U.

24 **Thermo-oxidative Oligomerization of Aromatic Diamine**

B. A. Zaitsev L. G. Kleptsova I. D. Shvabskaya A.E. Bursian

BILINGUAL PUBLISHING CO.
Pioneer of Global Academics Since 1984

Organic Polymer Material Research
https://ojs.bilpublishing.com/index.php/opmr

ARTICLE

AC Impedance and FTIR Studies of PVA-$ZnCl_2$ Based Solid Polymer Electrolytes

Jayanthi S*

The Standard Fireworks Rajaratnam College for Women (Autonomous), Sivakasi, 626123, India

ARTICLE INFO

Article history
Received: 14 August 2021
Accepted: 15 September 2021
Published Online: 15 October 2021

Keywords:
Complexation
FTIR
Ionic conductivity
Polymer electrolytes

ABSTRACT

Solid Polymer electrolytes (SPEs) comprising of poly(vinyl alcohol) (PVA) added Zinc chloride ($ZnCl_2$) systems have been prepared via solvent casting technique. The prepared samples have been subjected to AC impedance spectroscopic analysis and Fourier Transform Infrared Spectroscopy (FTIR) studies. Maximum ionic conductivity of $3.91949*10^{-7}$ Scm^{-1} was achieved for 60 wt% of PVA and 40wt% of $ZnCl_2$ system at room temperature. The structural changes and hence the complex formation between the constituents used in the present study has been confirmed through FTIR analysis.

1. Introduction

The possible application of solid polymer electrolytes (SPEs) in a diversity of electrochemical appliances rises from their advantages such as high energy density, electrochemical stability and easy handling. Solid polymer electrolytes are more suitable because they have improved shape, easy to handle, and possibilities for electrolytes leaking are none [1].

Poly(vinyl alcohol) (PVA) has excellent film forming nature, high tensile strength and flexibility. It is a crystalline, synthetic water- soluble polymer and has very important application due to the role of hydroxyl groups and hydrogen bands assist in the formation of polymer blends. It has some technological advantages in electrochemical devices, fuel cells, etc [2]. All these appealing characteristics made us choose PVA.

Most of the polymer electrolytes developed by researchers are of lithium based on. But the lithium salts have some negative factors, i.e they are i) scarcely available, ii) not safety, iii) high cost. To alleviate these issues, it is needed to choose the alternate to lithium salts. Keeping this in mind, many reporters developed the SPEs with the help of sodium [3], zinc [4], potassium [5] and magnesium [6], which act as an ionic source to the polymers. Of these above, the zinc added polymer system

**Corresponding Author:*
Jayanthi S,
The Standard Fireworks Rajaratnam College for Women (Autonomous), Sivakasi, 626123, India;
Email: jayanthi-phy@sfrcollege.edu.in

DOI: https://doi.org/10.30564/opmr.v3i1.3561

has revealed greater interest compared to others.

The devices which are based on Zinc possess higher specific and volumetric energy density. Also, this system has a comparable ionic radius of Li^+ (68 pm) and Zn^{2+} (74 pm). Therefore, we may use zinc as an insertion compound instead of lithium ions. Literature study reveals that the polymer electrolyte system based on zinc are very less. Hence, it has been decided to prepare zinc based polymer electrolyte system. For the present work, we have chosen a very simple electrolyte, zinc chloride as it is very cheap, easily available and can handle easily in atmosphere.

The present work deals with the preparation and characterization of polymer electrolytes based on PVA with $ZnCl_2$ by solution casting technique using distilled water as solvent.

2. Materials and Methods

Polymer films, PVA:$ZnCl_2$ of different compositions have been prepared using solution casting technique. First PVA is dissolved in distilled water and it was stirred well. After complete dissolution of PVA different concentrations of $ZnCl_2$ is added in the same solution and this mixture was stirred well until a homogenous solution was obtained. Then, the homogenous solution has been poured in the propylene petri dishes and allowed to evaporate in hot air oven at 60°C. From this experiment we attained a stable free standing films.

3. Characterization Techniques

3.1 AC impedance Analysis

Impedance values of the SPEs were determined with the help of Hioki impedance analyzer in the frequency range of 1 Hz – 5 MHz with a signal amplitude of 2mV using stainless steel blocking electrodes.

3.2 FTIR Analysis

The FTIR spectra were recorded using SHIMADZU FTIR spectrophotometer in the wave number region 4000 – 400 cm^{-1}.

4. Results and Discussion

4.1 AC Impedance Analysis

AC impedance plot of PVA & $ZnCl_2$ system is given in Figure 1. It contains of two clear regions, a depressed semicircle in the high frequency region and a slanted spike in the low frequency region. The semicircular portion correlates to the parallel combination of bulk resistance and capacitance. Further the semicircle which is semicircle in nature divulges the non-Debye nature of the sample owing to the potential well for each site, through which transportation of ion takes place [7].

The presence of slanted spike at low frequency region is at angle less than 90°. This is due to the roughness of the electrode-electrolyte interface.

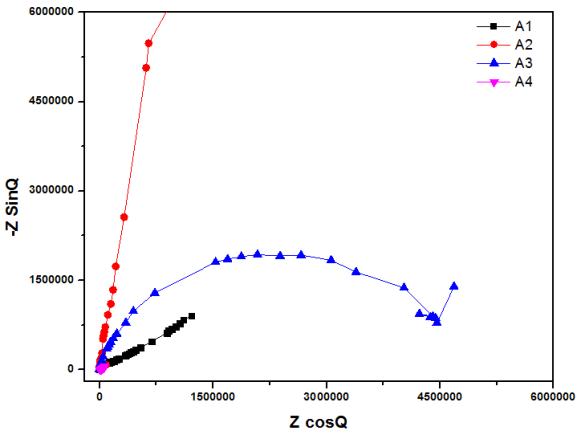

Figure 1. AC impedance plot of PVA - $ZnCl_2$ system

The intercept of the low-frequency spike at the real axis of the complex impedance plot gives the value of R_b.

The ionic conductivity (σ) of $BaTiO_3$ added polymer electrolyte system is calculated with the help of following equation

$$\sigma = \frac{l}{R_b A} \quad (1)$$

where, l represents the thickness of the prepared films, is the area of the SS electrode and is the bulk resistance.

The calculated values of ionic conductivity for PVA-$ZnCl_2$ system using Wquation (1) are given in Table 1. It is observed from the Table 1, that the value of ionic conductivity (σ) decreases against the increase of the concentration of $ZnCl_2$ from 10wt% to 30wt% in steps of 10wt%. The lesser value of ionic conductivity for 10, 20 and 30 wt% $ZnCl_2$ added system may be related to the re-association of the ions which leads to the formation of ion cluster of $ZnCl_2$ in the PVA matrix [2].

Table 1. Values of ionic conductivity PVA-$ZnCl_2$ system

Sample	PVA : ZnCl2 (wt%)	Ionic conductivity (Scm-1)
A1	90:10	2.5037×10^{-8}
A2	80:20	1.0079×10^{-9}
A3	70:30	1.0890×10^{-9}
A4	60:40	3.9194×10^{-7}

When the concentration of $ZnCl_2$ increased from 30wt% to 40%, an increase in the ionic conductivity is

observed. At 40wt%, the ionic conductivity reaches a maximum value of 3.9194 x 10^{-7}Scm^{-1} which is greater by two orders of magnitude when compared with the value 2.5037 x 10^{-8} Scm^{-1} of PVA-$ZnCl_2$ (90:10) system at room temperature. This enhancement in ionic conductivity can be related to the increase in the number of mobile charge carriers [8]. The film was fragile in nature when the concentration of $ZnCl_2$ was beyond 40%. Hence, the maximum ionic conductivity of 3.9194 x 10^{-7} Scm^{-1} is obtained for PVA-$ZnCl_2$ (60:40) system.

4.2 FTIR Analysis

The FTIR spectra of pure PVA, $ZnCl_2$ salt and PVA complexed with $ZnCl_2$ salt are shown in Figure 2. The following spectral changes are observed on comparing the spectra of complexed polymer electrolyte films with those of pure PVA and $ZnCl_2$ salt.

The pure PVA has a broad peak in the range 3757–3078 cm^{-1} pertains to O-H stretching [9]. The wideness of the peak is accredited to the intra and/or intermolecular hydrogen bonding [10], and the same is found to be present for $ZnCl_2$ added PVA systems. C-H stretching of CH_2 showed a peak 2924 cm^{-1} for pure PVA [10] and is slightly shifted to 2916 cm^{-1} in 20% and 30% weight percentage of $ZnCl_2$ added systems respectively, whereas there is no shift for another weight percentage systems.

The characteristic vibrational band at 1257 cm^{-1} corresponds to C=O stretching of secondary alcohols [10] and is shifted to 1242 cm^{-1} in the complexed polymer electrolyte film. C = C stretching occurring at 1111cm^{-1} in pure PVA is shifted to 1121cm^{-1} for $ZnCl_2$ added systems. All these changes in the FTIR spectra confirm the complexation between PVA and $ZnCl_2$.

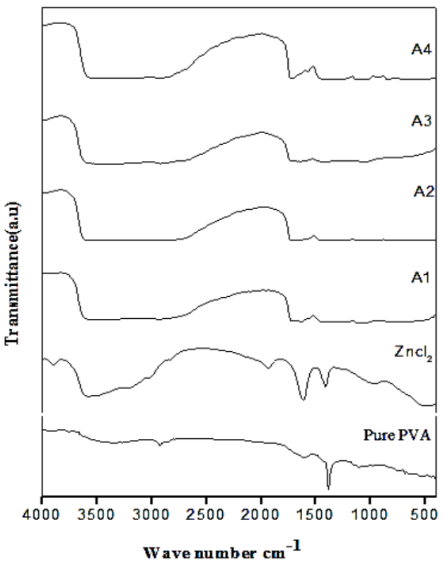

Figure 2. FTIR spectra of PVA with $ZnCl_2$ system

5. Conclusions

In this work, the structural and electrical properties of the solid polymer electrolytes based PVA and $ZnCl_2$ via solution casting technique have been studied. Maximum ionic conductivity of 3.91949 x 10^{-7} Scm^{-1} was observed for (60:40) PVA:$ZnCl_2$ system at room temperature. FTIR analysis reveals the possible bonding present in the polymer - salt complex and confirms the complex formation between the polymer and the salt.

References

[1] S. Jayanthi, B. Sundaresan, Influence of nano $SrTiO_3$ and ultrasonic irradiation on the properties of polymer blend electrolytes, Polymer-Plastics Technology and Materials 59 (2020) 2050. DOI: https://doi.org/10.1080/25740881.2020.1784220.

[2] K. Sundaramahalingam, K. Karpagavel, S. Jayanthi, D. Vanitha, N. Nallamuthu, E. R. Nagarajan, Structural and Electrical behaviours of amino acid-based solid polymer electrolytes, Bulletin of Materials Science 44 (2021) 196. DOI: https://doi.org/10.1007/s12034-021-02464-9.

[3] S. Jeya, S. Jayanthi, A. Arulsankar, B. Sundaresan, Enhancement of ionic conductivity of poly (vinylidene fluoridehexafluoropropylene) based solid polymer electrolyte by the incorporation of 1-methyl-3-propylimidazolium iodide, International Journal of Chem Tech Research 6 (2014) 5208.

[4] G. Girish Kumar, S. Sampath, Spectroscopic characterization of a gel polymer electrolyte of zinc triflate and polyacrylonitrile, Polymer 45 (2004) 2889. DOI: 10.1016/j.polymer.2004.02.053.

[5] S. Jayanthi, A. Arulsankar, G. P. Kokila, S. Banulakshmi, B. Sundaresan, FTIR, XRD and AC impedance studies of the polymer electrolyte PEMA – KSCN added with $SrTiO_3$, International Journal of Chem Tech Research 6 (2014) 5366.

[6] V. Aravindan, G. Karthikaselvi, P. Vickraman, S. P. Naganandhini, Polyvinylidene fluoride-based novel polymer electrolytes for magnesium-rechargeable batteries with $Mg(CF_3SO_3)_2$, Journal of Applied Polymer Science 112 (2009) 3024. DOI: 10.1002/app.29877

[7] S. Jayanthi, Studies on ionic liquid incorporated polymer blend electrolytes for energy storage applications, Advanced Composites and Hybrid Materials 2 (2019) 351. DOI: 10.1007/s42114-019-00102-x

[8] M. Ulaganathan, S. Rajendran, Li ion conduction on plasticizer-added PVAc-based hybrid polymer electrolytes, Ionics 16 (2010) 667-672. DOI: 10.1007/

s10800-010-0211-x

[9] M. A. Jothi, D, Vanitha, S. A. Bahadur, N. Nallamuthu, Promising biodegradable polymer blend electrolytes based on cornstarch:PVP for electrochemical cell applications, Bulletin of Materials Science 44 (2021) 65. DOI: https://doi.org/10.1007/s12034-021-02350-4.

[10] M Anandha Jothi, D Vanitha, S Asath Bahadur, N Nallamuthu, Investigations of biodegradable polymer blend electrolytes based on Cornstarch: PVP: NH_4Cl and its potential application in solid-state batteries, Journal of Materials Science: Materials in Electronics 32 (2021) 5427. DOI: 10.1007/s10854-021-05266-1

BILINGUAL PUBLISHING CO.
Pioneer of Global Academics Since 1984

Organic Polymer Material Research
https://ojs.bilpublishing.com/index.php/opmr

ARTICLE

Development of NR/SBR Based Rubber Compounds with Low Hysteresis and High Durability for Transmission V-Belts Applications

Asit Baran Bhattacharya[1,2] **M. Pandy**[1,2] **Kinsuk Naskar**[1*]

1. Rubber Technology Centre, Indian Institute of Technology, Kharagpur, 721302, India
2. J. K. Fenner (India) Ltd., Madurai, 625016, India

ARTICLE INFO

Article history
Received: 16 August 2021
Accepted: 15 September 2021
Published Online: 15 October 2021

Keywords:
Rubber
V-Belts
Power Transmission
NR
SBR
Fatigue
Failures

ABSTRACT

Power transmission by the belts is defined as, the transmission of power by a moving pulley to one or more driven machines through a flexible non-metallic member. There are different types of V-belts available, and Transmission Belts are one of them. Transmission V-Belt is the first invented non-metallic belts. Nowadays V-belts are used in various conditions, especially high-power transmission. These V-belts are finding their importance in many heavy industries. One of the good features of this type belt is no slippage occurs during the run. NR and SBR have used elastomers and can act as a base rubber material for this purpose. This study includes the compounding improvement for transmission V-Belts with NR and SBR rubber blends. There were so many numbers of failures in different ways during the initial research. Product failure methods and effect analysis (PFMA) have done by testing the belts multiple times and it has found that the major factors for the failure and less durability were excessive heat build-up (HBU) and poor fatigue resistance, poor crack initiation and growth, the resistance of the materials. So, initially reduction of HBU has successfully made in many steps by studying the properties of various compounds with a different type of fillers combinations, rubber combinations, curing systems variations etc. We have also improved the adhesion strength with cord and fabrics. Initially, we have taken one compound showing better properties in all aspects and have taken Belt Trial. And after some more improvement, we have found a compound showing better properties in all the cases than first trial and regular trials. By using that compound, we have developed Belts and showing better durability than earlier experiments and regular production.

**Corresponding Author:*
Kinsuk Naskar,
Rubber Technology Centre, Indian Institute of Technology, Kharagpur, 721302, India;
Email: knaskar@rtc.iitkgp.ernet.in

DOI: https://doi.org/10.30564/opmr.v3i1.3568

1. Introduction

In the last few decades, the popularity of rubber belts or rubber v-belts for power transmission is increasing widely in original equipment manufacturer (OEM) and also in the aftermarket. Power transmission by belts is described as the transmission of power from the prime mover to one or more driven machines by means of a flexible non-metallic member. That non-metallic member is generally a number of layers of various rubber compounds that are reinforced with cords and textiles. Basically, transmission belts shall consist of a combination of fabric, cord and elastomeric compounds, the whole being bonded together in a uniform manner and shaped in accordance with the best manufacturing practice.

As the market demand is increasing extensively, so many research and development works on belt design and compound design are also increasing. Not only the compound designing but also the tension member is important for better performance. Now a day's polyester, aramid and glass cord fibres are getting much importance for those purpose. There are so many layers in the belt (Figure 2). It is very difficult to identify the influences in the belt performance. That's why initially we have focused on rubber compound.Few major technical characteristics of the rubber compounds of the V-Belts are - (1) it should have good mechanical strength, (2) Least heat generation or heat build-up, (3) Good heat resistance, (4) Excellent resistance to flex cracking.

There are a wide variety of factors encountered in various types of belts responsible for belt life and abnormal failure. If we can increase the heat resistance or decreasing the HBU during applications, life can be improved. Another main factor is fatigue life improvement. According to Mars *et al.* [1], there are so many factors that affect the fatigue crack nucleation and growth process in rubber.

The rubber compound should have very good fatigue life as well as low heat build-up. Therefore, NR and SBR are widely used as raw rubber, for these applications. Because NR has very good mechanical strength and good tackiness and in the other hand SBR also having good mechanical strength, very good crack initiation resistant property. One of the most important points to note here is the adhesion problem between different rubber layers, between cord and rubber and between fabric and rubber layers. Especially for belts adhesion between different layers should be very good.

In the literature, there are some solutions when we

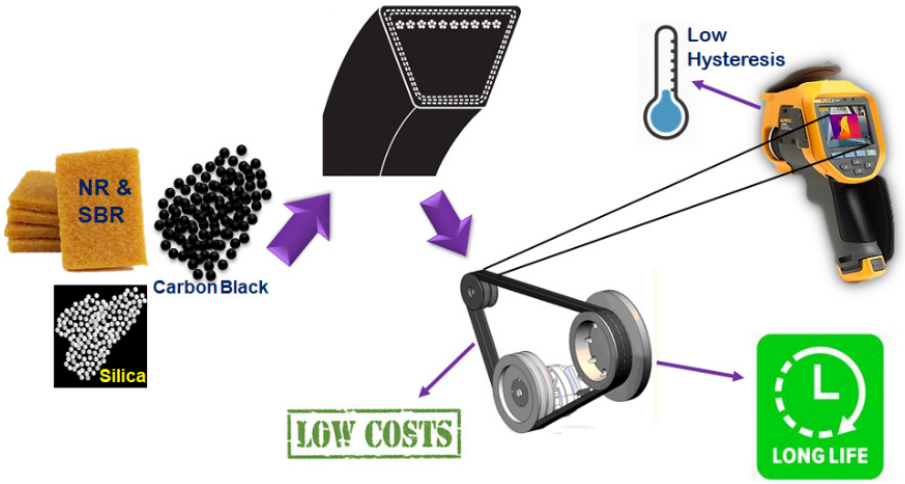

Figure 1. Power transmission

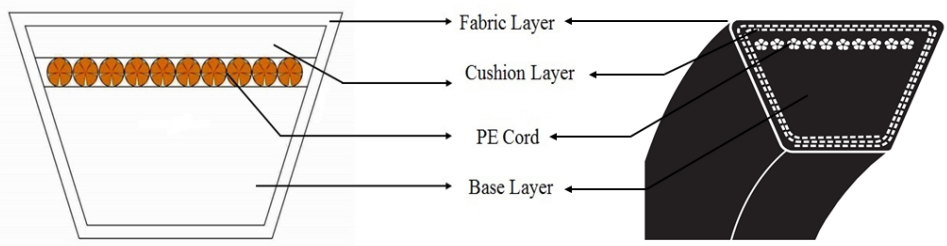

Figure 2. Cross-section of a Transmission V-Belt

looked into material studies, especially for V-belts.Among of those studies, the various mechanical properties of V Belt rubber compounds and compared with some others rubber products. In this work, we can get a brief study of NR based compound for V-belt and tyre. In another research work, the effect of temperature on fatigue life of V-ribbed serpentine belts has reported [2]. Fatigue crack growth model has proposed by them by finite element analysis. In 1996, Anil K. Bhowmick and Kamal K. Kar studied the hysteresis loss in filled rubber vulcanizates and its relationship with heat generation in Natural Rubber and SBR [3]. Sundararanman*et al.*studied the fatigue crack growth analysis of V-ribbed belts using finite element analysis in 2007 [4]. Wongwitthayakool*et al.* made a review on prediction of heat build-up behaviour on carbon black filled rubber [5]. Jun Liu *et al.*made a Numerical simulation and experimental verification of heat buildup for rubber compounds in 2015 [6]. G. Song and K. Chandrashekhara made a review on cord reinforcement properties of V-Belts with thermal effects and published some hyper-elastic models and Finite element analysis in 2005 [7]. Milan S. Banic and S. Stamenkovi predicted the heat generation behaviour of rubber due to hysteresis losses and low rubber thermal conductivity [8]. C. Rajesh and G. Unnikrishnan studied cure characteristics and mechanical properties of short nylon fibre-reinforced elastomers but with NBR [9]. In 2010 V. Le Saux and Y. Marco studied an energetic criterion for the fatigue of rubbers: an approach based on a heat build-up protocol and µ-tomography measurements [10]. A. Andriyana*et al.* studied on prediction of fatigue life improvement in natural rubber using configurationally stress in 2007 [11].

2. Experimental

2.1 Materials

Natural Rubber (ISNR Grade) which has used in all blend groups, has a Mooney Viscosity [80±5 ML(1+4) at 100ºC]. SBR (Non Staining Emulsion Grade) also used in all blend groups, has a Mooney Viscosity [55±5 ML(1+4) at 100ºC], bound styrene content 23.3%, procured from Kumho Petrochemical. Polybutadiene Rubber (PBR) used in all blend groups, has a Mooney Viscosity [45±5 ML(1+4) at 100ºC], Cis-1,4 content 96%, procured from Reliance Industries Limited. Three different types of carbon black we have used procured from PCBL, as a reinforcing filler in all the formulations. Others chemical were procured from regular sources, like Anti-oxidants, Vulcanising Accelerators (CBS, MBTS, TMTD) from NOCIL.

Table 1. Formulations of the Compounds in phr*

Ingredients	C-CB						C-RR				
	1	2	3	4	5	6	1	2	3	4	5
NR	100	0	55	55	55	55	**45**	**40**	**35**	**35**	**30**
SBR	0	100	45	45	45	45	**55**	**60**	**60**	**55**	**55**
BR	0						**0**	**0**	**5**	**10**	**15**
Silica	5.0						15				
HAF Black	**20**	**20**	**25**	**25**	**30**	**30**	25				
FEF Black	**50**	**50**	**50**	**45**	**40**	**35**	35				
SRF Black	**15**	**15**	**15**	**20**	**20**	**25**	20				
Resin A	3.0										
Sulphur	2.7										
CBS	2.5										
TMTD	0.2										

Table 2. Formulations of the Compounds in phr*

Ingredients	C-CS							CF		
	1	2	3	4	5	6	7	1	2	3
NR	35.0									
SBR	55.0									
BR	10.0									
Silica	15.0									
HAF Black	25.0									
FEF Black	35.0									
SRF Black	20.0									
Resin A	3.0							**2.0**		
Resin B	0.0							**2.0**		
Sulphur	**3.5**	**2.7**	**3.5**	**2.7**	**2.7**	**2.7**	**2.7**	2.7	2.7	2.7
CBS	**2.4**	**0.0**	**0.0**	**2.5**	**2.3**	**1.8**	**1.3**	1.3	1.3	1.3
MBTS	**0.0**	**2.4**	**2.5**	**0.0**	**0.0**	**0.0**	**0.0**	0.0	0.0	0.0
TMTD	**0.2**	**0.2**	**0.2**	**0.2**	**0.2**	**0.3**	**0.2**	0.2	0.2	0.2

*phr - Parts per hundred grams of rubber

2.2 Preparation of the Compounds

All the blend compounds were mixed in lab size two roll mills (Bharaj Rubber Processing Machineries, Thane, India). We have followed the following sequence for all laboratory batches (Figure 3). The milling temperature was 100ºC and time for 20 mins. Mixing for bulk batches for the final product was done in an internal mixer (Shaw K4 intermixes).

2.3 Testing Procedure

2.3.1 Vulcanizate Property Study

Rheometric behaviour of all rubber blends was performed in Ektrontek EKT2005 Rheometer, China at 160°C for 15 mins according to the method described in ASTM D5289. Mooney Scorch values (125°C at 30 mins) were determined in Mooney Viscometer (MV2000 Mooney Viscometer), Alpha Technologies, Hudson, Ohio, USA. The testing procedure was followed according to the method described in ASTM 1646.

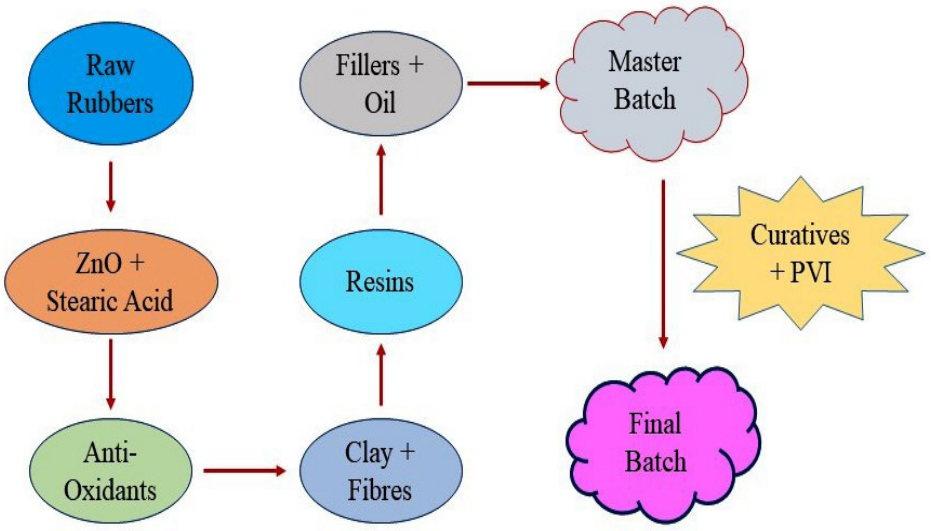

Figure 3. Scheme of preparation of blend compounds

2.3.2 Preparation of Samples and Mechanical Properties Study

The compounds were formed in sheets and were moulded in compression moulding machine (Santosh Industries, India) at 160°C for 15 minutes at 1000 psi pressure according to their respective curing time as per the ASTM standards. The hardness of each sample was measured by IRHD Durometer (Wallace Cogenix Hardness Tester) as per ASTM D 1415 test method. Average of three observations has taken. To study the different type of physical properties of the samples like Tensile strength, Elongation at break and Modulus, we have cut the Dumbbell sample according to ASTM D-412 from 2.5 ± 0.5 mm sheath and and same for Tear Strength according to ASTM D-624 and tested in Universal Testing Machine (Instron 3366). All the samples were aged in an aging oven (70°C for 70 hrs) and tested after that.

2.3.3 Heat Build-up (HBU) Measurement

Heat Buildup of the samples was tested as per ASTM D-623 in Goodrich Flexometer, operated under constant frequency 30 Hz, stress 2 kPa and stroke 1800 cycles/min.

2.3.4 Fatigue Property Study

To determine the dynamic properties of the rubber sample DeMattia Fatigue test are widely followed in industries. Respective samples were prepared by compression moulding and tested according to ASTM D-813 specifications by using DeMattiaFlexometer. Usually, the length of propagation of the crack was measured for every 30 min. An average of three samples was taken for the account.

2.3.5 Characterizations of the Samples

DMA was done in Metravib DMA-50 to measure the tanδ (loss factor) of the rubber compounds in temperature sweep at a constant frequency 1 Hz in tension mode having 2 mm thickness, 5 mm width and 25 mm length of the samples.

Thermal stability of the compounds was characterized by Thermal Gravimetric Analyser (Shimadzu TGA-50) at a temperature range of ambient temperature to +650ºC at N_2 atmosphere at 10 K/min heating rate.

3. Results and Discussions

3.1 Compound Series: 1

The following Table 3 shows the mechanical properties of the samples before and after aging. If tensile strength is the only concern, then CCB02 (100% SBR) would be the best one. But, 100 % SBR compound will be more costly than regular compound, that's why we are not considering that compound for the next step. And, according to our application, all mechanical properties are highly considered; in that case, CCB04 is the best compound.

In the other hand we can see that, Compression Set% also least for the compound CCB04 than other compounds. We have considered this compound for the reference compound in the next trials.

3.2 Compound Series: 2

In this trial, we have taken the Carbon Black percentages of the compound CCB04, NR and SBR blend compound (HAF: FEF: SRF = 25:45:20) which

Table 3. Mechanical properties of the compounds before and after aging

Sample Name	Condition	T.S. in MPa	Retention of TS in %	E B %	Modulus in MPa			Hardness (IRHD)
					50%	100%	200%	
C-CB01	Initial	12.4	92	262	2.7	4.9	9.9	80
	Aging	11.4		194	3.5	6.5	11.5	80
C-CB02	Initial	14.8	100	242	3.1	6.0	12.9	81
	Aging	14.8		187	4.0	7.9	-	84
C-CB03	Initial	13.8	99	254	3.1	5.7	11.8	82
	Aging	13.6		182	4.2	8.0	-	83
C-CB04	Initial	14	97	273	2.6	5.1	11.0	80
	Aging	13.6		197	3.6	7.1	8.6	81
C-CB05	Initial	13.5	93	240	3.0	5.8	12.3	81
	Aging	12.6		156	4.2	8.3	-	84
C-CB06	Initial	13.3	96	237	3.0	5.6	11.8	84
	Aging	12.8		169	4.1	7.8	-	83

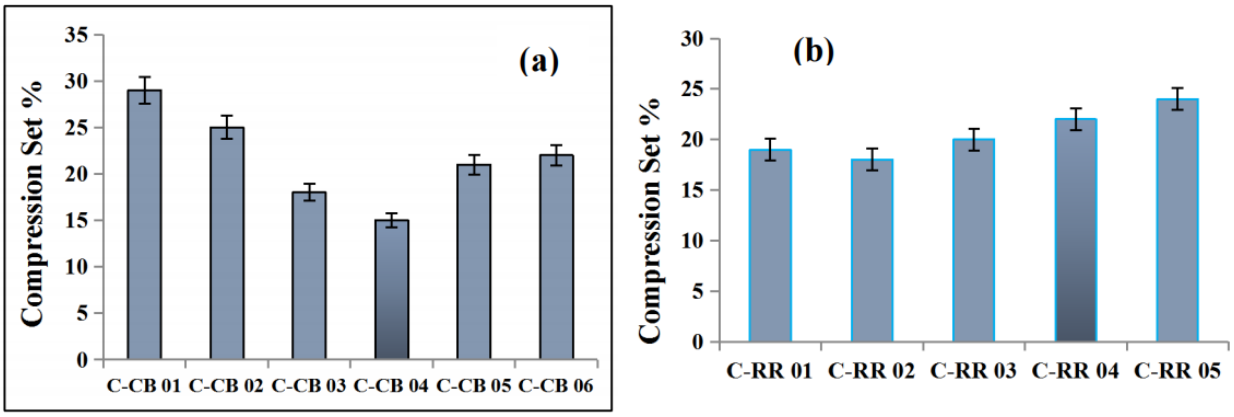

Figure 4. Compression Set % of the Compounds (a) and (b)

shows very good physical properties. We had replaced some amount of carbon black by Silica to improve the mechanical properties and also NR by Polybutadiene (BR) rubber to reduce Heat Buildup. From the Table 4, we can see that compound CRR04 is showing very good mechanical properties as well as Hardness also. In the case of compression set%, it is good for other compounds (Figure 4b). As mechanical properties are prime concern that's why compound CRR04 we have taken for reference compound in the next step.

3.3 Compound Series: 3

3.3.1 Compound Series: 3.a

In this trial, we have taken the Raw Rubber percentages of the compound CRR04 of NR-SBR-BR blend compound with the filler combination of HAF: FEF: SRF = 25:35:20 of earlier best combination (CCB04). Here, for two compounds CCS01 and CCS02, we have used the CV System and for C-CS03 and C-CS04 SEV System. For the first two compounds we have used CBS and TMTD combination and for the second two compounds, we have used MBTS and TMTD combination.

We can see that CCS01 and CCS04 showing good tensile strength and hardness but Elongation at Break is very less than CCS04 for CCS01. And also, we can see that Compression Set % is also higher for CCS01. That's why we are not considering that compound CCS01. For further confirmation, we have studied the Heat Build-up study which is discussed later.

Table 4. Mechanicalproperties of the compounds before and after aging

Sample Name	Condition	TS in MPa	Retention of TS in %	E B %	Modulus in MPa			Hardness (IRHD)
					50%	100%	200%	
C-RR01	Initial	14.7	101	269	2.7	5.2	11.5	82
	Aging	14.8		216	3.5	6.6	14.0	81
C-RR02	Initial	12.8	119	209	3.1	5.8	11.6	83
	Aging	15.2		225	3.6	6.8	14.0	80
C- RR03	Initial	14.7	97	213	3.3	6.3	13.2	82
	Aging	14.3		188	3.7	7.7	15.0	83
C-RR04	Initial	14.7	98	217	3.5	6.8	13.9	83
	Aging	14.4		160	4.1	8.2	-	83
C-RR05	Initial	14.5	97	239	3.0	5.8	12.4	82
	Aging	14.1		178	4.1	8.1	-	82

Table 5. Mechanicalproperties of the compounds before and after aging

Sample Name	Condition	TSin MPa	Retention of TS in %	E B %	Modulus in MPa			Hardness (IRHD)
					50%	100%	200%	
C-CS01	Initial	14.5	100	173	4.3	8.6	0.0	88
	Aging	14.4		145	5.0	10.1	0.0	87
C-CS02	Initial	14.9	94	216	3.5	6.8	14.1	86
	Aging	14.0		173	4.0	7.6	0.0	85
C-CS03	Initial	12.5	100	152	4.0	7.9	0.0	84
	Aging	12.7		143	4.0	8.4	0.0	82
C-CS04	Initial	14.0	103	246	3.1	5.8	12.4	86
	Aging	14.5		214	3.5	6.8	13.8	86

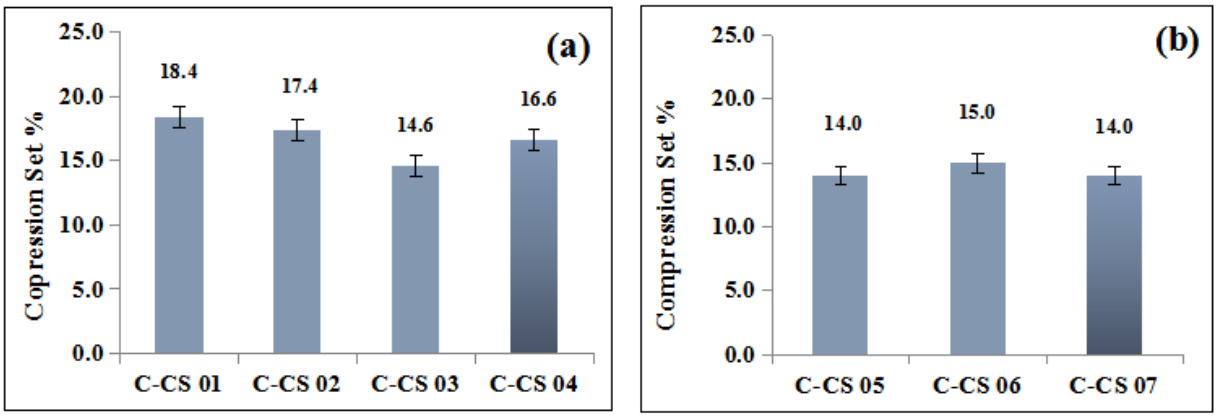

Figure 5. Compression Set % of the Compounds (a) and (b)

3.3.2 Compound Series: 3.b

After studying the curing system variation batches, we fixed the Rubber, Filler and Curing System combination of compound C-CS04, because this compound meeting our required properties and also showing the least amount of Heat Buildup. Next trial, we have tried to observe the effect of the accelerator in different amounts. That's why we have taken three different amounts of CBS and by keeping the Sulfur and TMTD amount the same.

Table 6. Mechanical Properties of the compounds before and after Aging

Sample Name	Condition	TS in MPa	Retention of TS (%)	E B %	Modulus in MPa			Hardness (IRHD)
					50%	100%	200%	
C-CS05	Initial	13.1	92	209	3.4	6.0	11.8	85
	Aging	12.0		200	3.4	7.0	0.0	82
C-CS06	Initial	13.4	94	218	3.3	5.8	12.0	86
	Aging	12.6		210	4.0	7.5	0.0	85
C-CS07	Initial	13.8	94	264	3.0	5.1	10.8	87
	Aging	13.1		250	3.7	6.9	0.0	84

3.4 Compound Series: 4

In this trial, we have tried to increase the adhesion strength than regular compound and decreasing the Heat Buildup. We have optimized two different approaches - a) Using two different types of accelerator and variation in amount, i.e. Conventional and Semi-efficient, b) after optimization of the system (CV or SEV) we have tried to study the effect of the amount of accelerator with a constant amount of Sulphur and TMTD.

We have seen that SEV system with CBS+TMTD combination presenting least heat build-up and for next trials CCS07 is presenting least Heat Buildup than other compounds. That's why we have taken the curing system of the CCS07 for final trial batches.

Here we have taken two different of Resins to increase the adhesion strength between the compound and fabric and compound and cord. Previously we have used only one resin. And another variation we have made in these trials, we have varied the amount of Silica for increasing the strength and decreasing the Heat Buildup and we have decreased the total Carbon black amount from 80 to 75 PHR.

From the Table 7, we can see that CF01 and CF02 compounds are showing good Tensile Strength but CF03 showing less. As a reason may be, higher filler agglomeration presents in CF03 compound because of a higher amount of Silica. And it easily visible that, as

Table 7. Mechanical Properties of the compounds before and after Aging

Sample Name	Condition	TSin MPa	Retention of TS in %	E B %	Modulus in MPa			Hardness (IRHD)
					50%	100%	200%	
CF01	Initial	14.4	87	285	2.7	4.8	10.6	82
	Aging	12.5		188	3.6	7.1	-	82
CF02	Initial	14.7	88	277	2.9	5.3	11.3	83
	Aging	12.9		168	3.9	7.6	-	83
CF03	Initial	13.2	94	263	2.9	5.1	10.6	85
	Aging	12.4		176	3.9	7.3	-	86

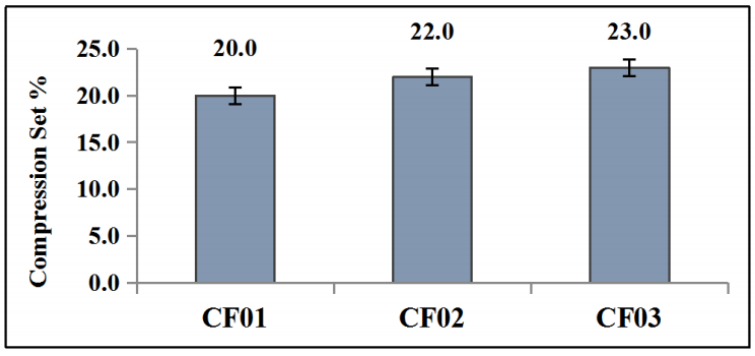

Figure 6. Compression Set % of the Compounds

the amount of Silica increased, Elongation at Break also decreased.

In the other hand Modulus (50%, 100%, and 200%) and Hardness (IRHD) is not varied significantly with respect to the other properties.

After studying the above three compounds we can observe that with the respect of Mechanical properties CF01 compound is showing the best properties. And if see Compression Set % and Abrasion Resistance, that also best for CF01 compound. And the other properties like Heat Build-up and Fatigue resistance, have discussed later.

3.5 Heat Build Up Results

We have studied Heat Build-up (ΔT in ºC) thoroughly for all the compounds results are as follows.

Table 8. Compound Series #1 (C-CB)

	0 Min	5 Min	10 Min	15 Min	20 Min	25 Min
C-CB 01	52	19	23	24	25	25
C-CB 02	52	21	24	25	26	26
C-CB 03	52	19	23	24	25	26
C-CB 04	52	18	22	23	23	**24**
C-CB 05	52	21	26	26	27	27
C-CB 06	52	21	26	27	27	27

Table 9. Compound Series #2 (C-RR)

	0 Min	5 Min	10 Min	15 Min	20 Min	25 Min
C-RR 01	52	15	21	21	22	24
C-RR 02	52	16	20	21	22	24
C-RR 03	52	19	23	25	25	25
C-RR 04	52	17	21	22	22	**22**
C-RR 05	52	21	24	24	24	24

Table 10. Compound Series #3 (C-CS)

	0 Min	5 Min	10 Min	15 Min	20 Min	25 Min
C-CS 01	52	19	22	24	24	24
C-CS 02	52	19	23	24	24	24
C-CS 03	52	19	23	24	24	24
C-CS 04	52	19	21	22	22	**22**
C-CS 05	52	19	22	23	24	24
C-CS 06	52	19	22	24	24	24
C-CS 07	52	18	19	19	21	**22**

Table 11. Compound Series #4 (CF)

	0 Min	5 Min	10 Min	15 Min	20 Min	25 Min
CF 01	52	19	20	20	22	**22**
CF 02	52	19	21	23	24	24
CF 03	52	19	23	24	24	25

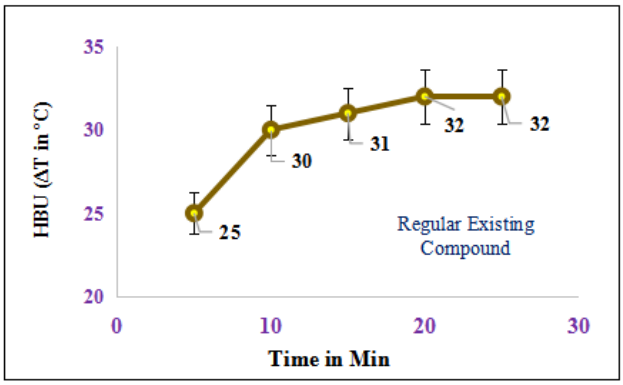

Figure 7. Heat Buildup of Regular Existing CompoundHeat Buildup decrease in percentage (%) than Regular Existing Compounds.

Table 12. Decreasing of HBUin % (ΔT at 25 min)

C-CB01	22	***C-RR01***	25	***C-CS01***	25	***C-CF01***	**31.3**
C-CB02	19	***C- RR02***	25	***C-CS02***	25	***C-CF02***	25
C-CB03	19	***C-RR03***	22	***C-CS03***	25	***C-CF03***	22
C-CB04	**25**	***C-RR04***	**31**	***C-CS04***	**31.3**	-	-
C-CB05	16	***C-RR05***	25	***C-CS05***	25	-	-
C-CB06	16	-	-	***C-CS06***	25	-	-
-	-	-	-	***C-CS07***	**31.3**	-	-

3.6 Adhesion Test Results

3.6.1 Fabric Adhesion Strength (180º Pell Test) [ASTM D3330]

Table 13. Fabric Adhesion Test Results

	Regular Compound	CF01	CF02	CF03
Strength in Lbf/in	11.21	17.12	14.80	19.27
Change in % w.r.t Regular Compound		**53**	**32**	**72**

3.6.2 Cord Adhesion Strength

Table 14. Cord Adhesion Test Results

	Regular Compound	CF01	CF02	CF03
Strength in kgf	4.37	5.76	3.42	4.39
Change in % w.r.t Regular Compound		**32**	**-22**	**0**

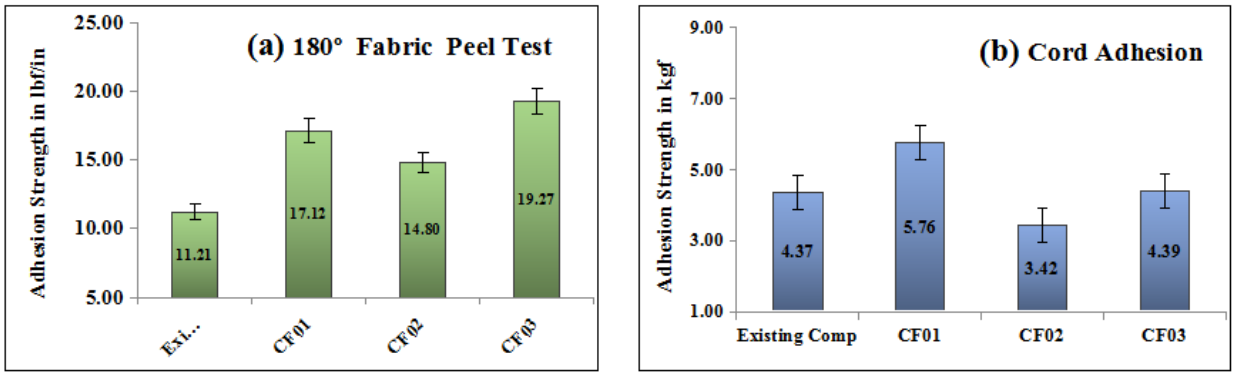

Figure 8. Adhesion Strength Comparisons of the Compounds (a) Fabric and (b) Cord

3.7 DeMattia Results

The DeMattia Fatigue Test results are as follows.

From the DeMattia Fatigue Study, we can see that the Regular Compound showing Fatigue Life of about 190 Kilocycles and from the first trial batch Compound C-CB04 showing highest Life of about 263 Kilocycles. In the next trials, we can see that life is improved than earlier batches and it has achieved up to 272 Kilocycles. After final trials, we can see that the maximum Fatigue life we have achieved 270 to 272 Kilocycles and whereas Regular Compound life is 190 Kilocycles. That means we have increased the Fatigue life up to 40% than Regular Compound.

3.8 DMA Results

From the Figure 20, we can see that tan δ value is

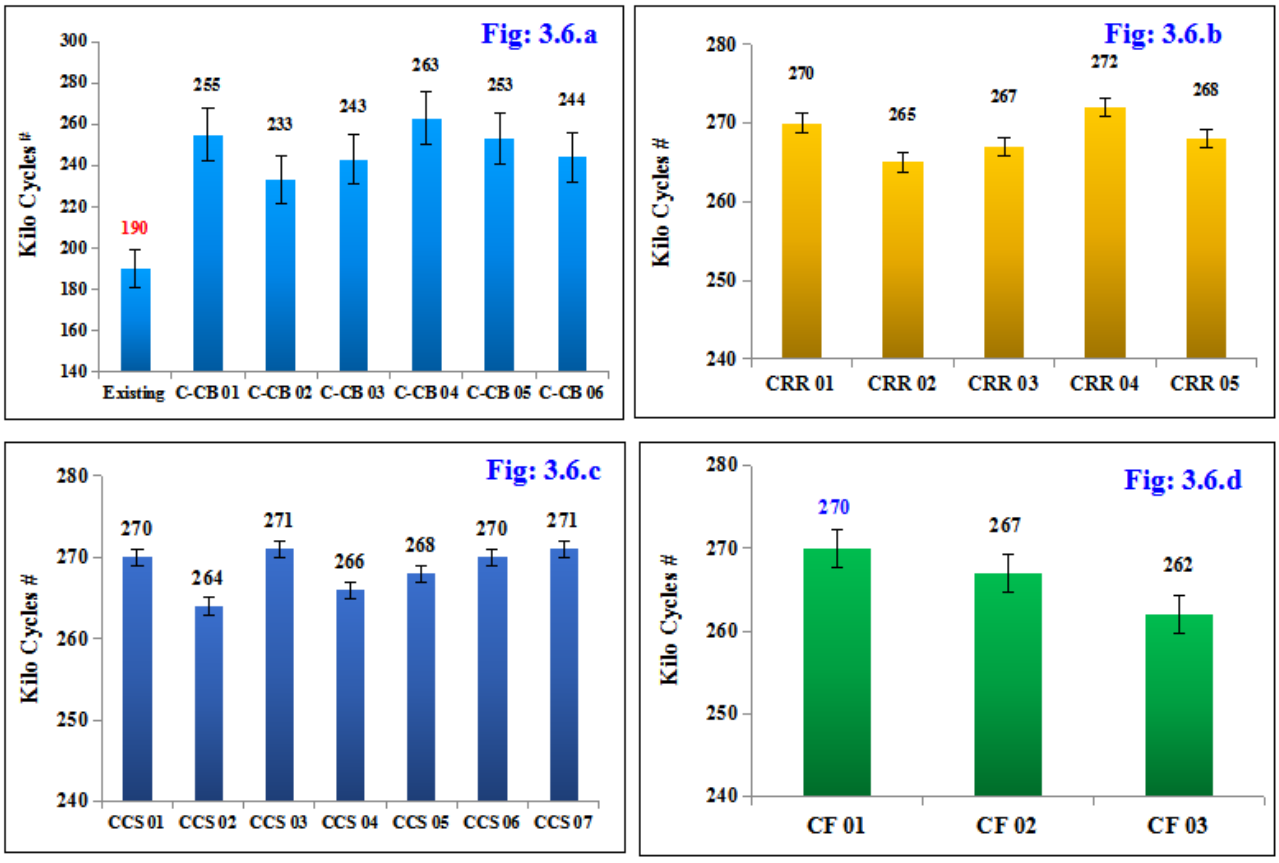

Figure 9. DeMattia Fatigue-Life of Compounds

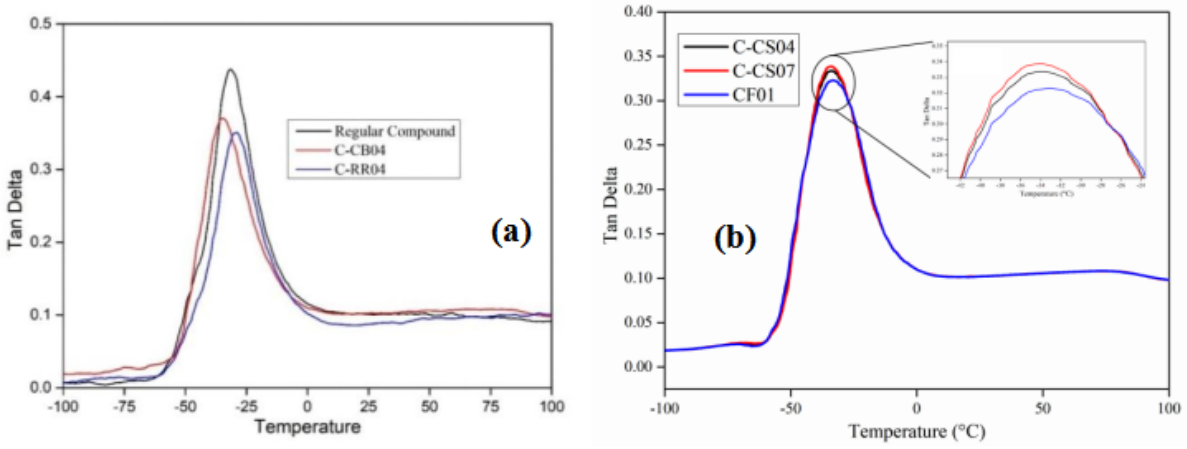

Figure 20. DMA Study of New compounds and Regular compounds

shifting downwards from Regular Compound > C-CB04 > C-RR04 and for Figure 20 we can see the same trend, C-CS04 > C-CS07 > CF01. That means Tanδ value decreasing and as the Tanδ value will be less Heat Buildup also will be less, which is in confirmation with the Heat Buildup data discussed earlier. In the above table, we have calculated the change tan δ with respect to Regular compound in percentage and we have decreased the tan δ value up to 14% to 24% less than Regular Compound.

Table 15. DMA Test Results Summary

Samples	Tan δ_{max}	Temperature	Change of Tan δ_{max} w.r.t. Regular Compound
Regular Compound	0.438	-31.68	-
C-CB 04	0.375	-34.84	14 %
C-RR 04	0.351	-29.04	20 %
C-CS 04	0.336	-33.78	23 %
C-CS 07	0.330	-34.14	24 %
CF 01	0.331	-33.25	24 %

3.9 Comparison: Regular and New Trials Bulk Batch Compound

Table 16. Comparisons of Different Properties

Parameters	Regular	New trial - I	New trial - II
Tear Strength in N/mm	54.69	58.84	61.9
Heat Buildup at 25 min	84	76	74
DeMattia Fatigue inKilo Cycles	190	258	270

3.10 TGA Results: Bulk Batch Compounds

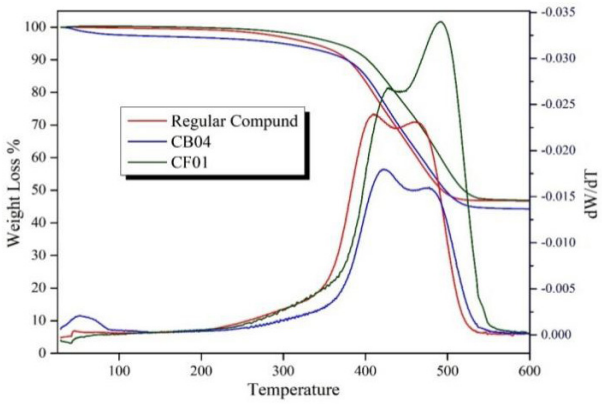

Figure 21. TGA Study of New compound and Regular compound

Table 17. TGA Results Summary

Compounds	Degradation Temperature	Change of Temperature w.r.t. Regular Compound
Regular	409ºC and 464ºC	-
New Trial - I (CB04)	425˚C and 477ºC	4 % and 3 %
New Trial - I (CF01)	439˚C and 492ºC	7 % and 6 %

From the above Figure 21 and Table we can see that we have got two degradation temperatures for all three compounds at a different temperature. We have also calculated the improvement or change in degradation temperature for New Trial compounds, and it is showing almost 6-7 % improvement.

3.11 Belt Physical Properties

From the below table, it is observed that our New Trials are showing good single cord adhesion strength than regular belts. Elongation at 160 Kgf, is also less than

regular belts. The Breaking strength of the belt per each cord is higher for our new trial than the regular belts.

Table 18. Belt Properties

	Regular Sample	New Trial 1	New Trial 2
Cord Adhesion	9.7	13.4	15.6
Improvement %	-	**38**	**61**
Jacket Adhesion	8.5	9.2	10.3
Improvement %	-	**8**	**21**
Breaking Strength	800	840	860
Improvement %	-	**5**	**8**

3.12 Durability Test at Test RIG

Table 19. Belt Durability

Type of Belts	Run without Crack in Hours	Run up to Failure in Hours	Durability Improvement in %	
Reg. Production	230	340	-	-
New Trial - I	283	**400**	**~23**	**~18**
New Trial - II	295	**415**	**~28**	**~22**

3.13 Belt Temperature Study at Test RIG

We have studied the belt temperature by Infrared Thermal Imager (FLUKE Ti480 PRO IR Camera) at a different time interval in same conditions, during running.

Figure 22. Belt Temperature Study by IR Thermal Imager

Table 20. Belt Temperature Generation

Type of Belts	Heat Generation at Side Portion
Regular Production	89ºC
New Trial - I	82ºC
New Trial - II	78ºC

4. Conclusions

We have done Heat Build-up study of all compounds with various fillers ratios, different rubber compositions, the effects of Curing Systems. The amount of reduction in HBU of C-CB04, C-RR04, C-CS04, C-CS07andCF01 compounds are 25%, 31%, 31.3%, 31.3% and 31.3% less, respectively than the Regular production compound. Finally, we tried to improve the adhesion strength between Compounds to Cord and Compound to Fabric. Fabric Adhesion improved 32-53 % than Regular Compounds. From the DMA study we can observe the Tanδ value of CF01 <C-CS07 <C-CS04 < C-RR04 < C-CB04 < Regular compound and this data trend is matching with the Heat build-up data trend. From the TGA study we can see that CF01 and C-CB04 are showing higher degradation temperature than a Regular compound. The developed New Trial-I and New Trial-II belts are providing 38% and 61% more cord adhesion strength and 5% and 8% more breaking strength, respectively than Regular compound belts. The New Trial-I and New Trial-II belts are giving nearly 60-70 hours more life than previous trials. We have measured the Belts Temperature during running condition and it is showing less temperature generation for New Trial Belts.

Acknowledgement

Authors also would like to thank J. K. Fenner (India) Limited, Madurai, Tamil Nadu, India, for giving me the opportunity to carry out the project in plant. Special thanks to Dr.TuhinChatterjee and DebabrataGanguly for their kind support. Also, thanks toSyadMushtaq, Dipankar Bhattacharya and ArunChanda for helping in experiments in the laboratory.

References

[1] W. V. Mars, A. Fatemi, 'Factors That Affect the Fatigue Life of Rubber: A Literature Survey', Journal of Rubber Chemistry and Technology, Vol. 77, No. 3, pp. 391-412, 2004.

[2] Sundararaman S., Saikrishna, "Mode-I fatigue crack growth analysis of V-ribbed belts." Finite Elements in Analysis and Design 43.11 (2007): 870-878.

[3] Kar, Kamal K., and Anil K. Bhowmick. "Hysteresis loss in filled rubber vulcanizates and its relationship with heat generation." Journal of Applied Polymer-Science 64.8 (1997): 1541-1555.

[4] Sundararaman, Saikrishna, "Temperature-dependent fatigue-failure analysis of V - ribbed serpentine belts." International Journal of Fatigue 31.8 (2009): 1262-1270.

[5] P. Wongwitthayakool, P. Saeoui, and C. Sirisinha, 'Prediction of heat build-up behaviour under high load by use of conventional viscoelastic results in

carbon black filled HNBR', Plastics, Rubber and Composites 2011 Vol 40 No 5.

[6] Fanzhu Li and Jun Liu, "Numerical simulation and experimental verification of heat build-up for rubber compounds",Polymer; Vol - 101(199-207); 2016.

[7] Chandrashekhara K.; ASME; Vol. 127, Nov-2005.

[8] Milan S. Banic, Dušan S. Stamenkovi, 'Prediction Of Heat Generation In Rubber Or Rubber-Metal Springs', Thermal Science, Year 2012, Vol. 16, Suppl. 2, Pp. S593-S606.

[9] Rajesh, C.; "Cure characteristics and mechanical properties of short nylon fiber-reinforced nitrile rubber composites." Journal of Applied Polymer Science 92.2 (2004): 1023-1030.

[10] V. Le Saux, Y. Marco, S. Calloch, P. Charrier, D. Taveau, 'Heat build Up of Rubber Under Cyclic Loadings: Validation of an Efficient Demarch to Predict the Temperature Fields', Rubber Chemistry and Technology, Vol. 86, No. 1, Pp. 38-56 (2013).

[11] Andriyana, E. Verron, 'Prediction of fatigue life improvement in natural rubber using configurational stress', International Journal of Solids and Structures.44 (2007) 2079-2092.

[12] Partha P. Sarkar, S.K. Ghosh, B.R. Gupta, and Anil K. Bhowmick, "Studies on adhesion between rubber and fabric and rubber and rubber in heat-resistant conveyor belt", International Journal of Adhesion and Adhesives, Vol.9 No.1 January 1989.

[13] Wallace D. Erickson, Belt Selection and Applications for Engineers by GATES Rubber Company; Marcel Dekker Inc.

[14] Anil K. Bhowmick, Malcolm M. Hall, Henry A. Benerey, Rubber Products and Manufacturing Technology by, Marcel Dekker, Inc.

[15] J. White, S. K. De, K. Naskar; Rubber Technologist's Handbook, Vol.-2 by, Rapra Technology Limited, 2009.

[16] Alan N. Gent, Engineering with Rubber, HANSER Publishers, 2012.

[17] J. B. Donnet, Carbon Black: Science and Technology, CRC Press, 1993.

BILINGUAL PUBLISHING CO.
Pioneer of Global Academics Since 1984

Organic Polymer Material Research
https://ojs.bilpublishing.com/index.php/opmr

ARTICLE

Impact of Mixed Fillers on the Physico-mechanical Properties of Flexible Polyether Foam

Onwuka, C.O. Anekwe, O. J. Ogudo, M.C. Chris-Okafor, P.U.*

Department of Pure and Industrial Chemistry, Faculty of Physical Science, Nnamdi Azikwe University, Awka, Anambra State, Nigeria

ARTICLE INFO

Article history
Received: 20 August 2021
Accepted: 15 September 2021
Published Online: 15 October 2021

Keywords:
Polyether foam
Periwinkle
African star apple seed shell
Mechanical properties
Scanning electron microscopy

ABSTRACT

The effect of proportional blend of periwinkle and African star apple seed shell as bio-fillers in flexible polyether foam was studied. Flexible polyether foam samples incorporated with these bio-fillers at varying percentages; 10% (S_1), 20% (S_2), 30% (S_3), 40% (S_4) and 50% (S_5) were produced respectively, while 0% (S_0) which had no filler was used as control during the experiment. The mechanical properties of the produced foam samples were determined via density, compression set, indentation hardness, tensile strength and elongation at break tests. The cream time, rise time and height of the foam as parameters for characterising the produced foam samples were determined too. Flammability test was also carried out. The microstructure of the foam samples was analysed as well by using the scanning electron microscope. The results of the experiment showed that the density of the foam samples progressively increased from 19.20 (S_0) – 26.45 (S_5) as the quantity of the filler increased. The indentation hardness result also showed an increase on addition of the filler. The foam's loading ability also increased on incorporation of the filler but S3 showed remarkable recovery after compression. The tensile strength and elongation at break of the foam decreased on addition of the filler. The morphological analysis ascertained the effect of the progressive introduction of the filler on the surface morphology of the foam. The flammability of the foam was found to decrease as the filler load increased. Since these fillers are of organic origin, readily available, cheap and eco-friendly, they provide a means of making biodegradable foam, and reducing the flammability of foam. Thus, reducing environmental pollution whilst enhancing the mechanical property of foam.

**Corresponding Author:*
Chris-Okafor, P.U.,
Department of Pure and Industrial Chemistry, Faculty of Physical Science, Nnamdi Azikwe University, Awka, Anambra State, Nigeria;
Email: pu.chrisokafor@unizik.edu.ng

DOI: https://doi.org/10.30564/opmr.v3i1.3604

1. Introduction

Polyurethane is any type of polymer containing urethane linkage. The urethane linkage is –NH-CO-O-. The polyurethane usually referred to as PU, is actually another name for the family of chemicals known as urethane polymers, which are composed of two principal raw materials: isocyanates and polyols, brought together with catalysts and a variety of additives [1]. Polyurethane might be hard like fiberglass, squishy like upholstery foam, protective like varnish, bouncy like rubber wheels or sticky like glue, I.e. it can exist as both rigid and flexible foams, since polyurethanes come in so many forms and can have a wide variety of properties, it therefore is used in many different applications [2]. The use of flexible polyurethane foams for cushions, furnishes, furniture and automobiles has displaced rubber foam in applications because of improved strength, lower density and easier fabrication [3].

The major raw materials used for the production of flexible polyurethane foam include Polymer Polyol, Isocyanate, Blowing agents, Catalysts, Surfactants and Additives such as Fillers which can be organic or inorganic [4]. These raw materials are mostly liquid reagents and chemicals obtained from petrochemicals and agro-products and hence the prices of flexible polyurethane foams are becoming increasingly high due to high cost of raw materials [5].

Fillers are used in the polymer matrices for various purposes such as to reduce cost, to reduce resin curing shrinkage, to control resin viscosity and to improve the stiffness and other properties of the matrix. Most commonly used filler materials in polymer matrix are calcium carbonate, alumina, and silicon carbide [6]. However, there is need for sources for renewable materials, which can serve as alternate fillers to the conventional mineral calcium carbonate ($CaCO_3$) which holds the largest market volume in the plastic section and is mainly imported. This gives room for developing countries to source out their own raw materials, reduce importation and enable the use of materials that are eco-friendly, non-toxic and biodegradable [7]. Natural fillers such as goat femur [8], egg shell [9], mixed coconut husk/corn cob [10] and rice husk/corn cob [11]. Snail shell among others has been considered as suitable substituent for inorganic fillers in polyurethane foams as a result of their various advantages [12].

Thus, this article reports an investigation on the mechanical properties, flammability and morphology of flexible polyether polyurethane foam filled with periwinkle and African star seed shell powder.

2. Materials and Methods

The quality of the end product in any manufacture process is dependent on the quality of the starting materials and the fact that manufacturing instructions are obeyed to the latter. Hence, it is pertinent to note that the raw materials used in the production of this work were sourced from Vitafoam Nigeria Plc. Bank Junction, Oba Akaran Industrial layout Ikeja, Lagos State, a company known to produce quality polyurethane materials such as pillows, mattress etc. since 1991.

Collection and preparation of periwinkle shell.

The periwinkle shells were obtained from Owerri, Imo state Nigeria. The periwinkle shells were first filtered by hand picking to remove other unwanted substances, washed thoroughly and allowed to dry for 96 hours. They were crushed to fine powder using an electric grinding machine. The crushed shells were further sieved using a muslin cloth with very small pores to obtain fine powder which had a particle size of 50 μm. It was stored in polythene bags.

Preparation of African star apple seed shell

The African apple star seed was sourced from Agulu, Anambra State, Nigeria. The seeds were then left to dry for 72 hours, so that the shell would come off easily from the seed-coat, the dry seeds were broken using a hammer and the shells were hand-picked, washed and dried for 48 hours and then crushed to fine powder using an electric grinding machine. After the crushing, the powder was sieved again to obtain smooth, fine textured powder with particle size of 50µm. it was stored in a polythene bag prior to the time of usage.

The periwinkle and African star seed shells were mixed in the ratio 50:50 and stored for production.

Foam formulation

The choice of the weights of raw materials to be used in foam production is not made arbitrarily. It is chosen on the basis of formulation. If high density foam is desired, the tendency is that the volume of water used will be reduced; this is due to the fact that density is universally related to volume [10].

Foam production

500g of the polymer polyol was poured into an empty clean plastic jug, 400g of each of the fillers; periwinkle shell and African star apple seed shell were weighed and mixed thoroughly to obtain a homogenous mixture

Table 1. Foam Formulation.

Raw materials	PPH	S_0 (g)	S_1 (g)	S_2 (g)	S_3 (g)	S_4 (g)	S_5 (g)
Polyol	100	500	500	500	500	500	500
TDI(index:1.08)	58.99	325	325	325	325	325	325
Water	4.36	28	28	28	28	28	28
Amine	0.422	2	2	2	2	2	2
Silicon oil	0.822	5	5	5	5	5	5
Tin catalyst	0.139	1	1	1	1	1	1
Filler(Periwinkle and African star apple seed shell)	---	0	50	100	125	200	250

Note: Pph = Part per hundred; S = sample; g = gram

containing 50% of each of the filler. 0g, 50g, 100g, 150g, 200g and 250g (0%, 10%, 20%, 30%, 40% and 50%) of the mixed fillers were weighed out respectively by using an electrical weighing balance of Model D-72336, Made in China. The quantities of the other raw materials were kept constant but the quantities of the fillers were varied according to the above percentage in each sample.

28g of water, 2g of amine, 5g of silicon oil and 1g of tin catalyst were carefully weighed out and poured into the plastic jug containing the polyol and to this mixture, the appropriate quantity of the mixed fillers for each sample was added. The mixture was stirred vigorously for 2 minutes, 325g of TDI was measured out in a separate beaker and added to the homogenous mixture and further stirring was done.

The mixture was transferred into a metal mould lined with brown paper; the brown paper was used to avoid the sticking of the foam to the body of the mould. The process was repeated for the different weights of the filler. Ten minutes after full rise was attained, the foam samples were removed from the mould and allowed to cure for 24 hours before characterization and testing. This was also repeated for the different foam samples based on their gram weight.

Characterization of the foam samples

The following mechanical properties of the foam samples were determined using standard methods: density, while tensile strength, elongation at break, compression strength and hardness test were measured according to the ASTM-D standard specifications [13]. The surface morphology of the sample was tested via Scanning electron microscope.

3. Results and Discussion

The results of the mechanical properties of the foam samples were observed. The percentage (%) compositions of periwinkle and African Star seed shells powder in each sample varying from 0% in Sample S_1 to 50% in sample S_5 at 10% interval. The foam properties studied and their corresponding results are as shown below.

Cream time, Rise time and Curing time

The result of the cream time, rise time and curing time recorded during production of polyurethane foam is shown in the Table 2.

Table 1. Observation during the experiment

Experiment	Cream time (secs)	Rise time (secs)	Curing time (secs)	Height (cm)
S_0	3	80	24	24.20
S_1	5	90	24	24.60
S_2	5	98	24	24.80
S_3	6	118	24	25.20
S_4	8	122	24	24.80
S_5	8	122	24	24.60

From Table 2, it was discovered that as the quantity of filler load increased, the time taken for the foam reaction to commence which is the cream time also increased. In the same vein, the time taken for the foam to attain maximum height also increased with increase in filler load. The height was regained as the filler load increased. This implies that there is a direct relationship between the cream time, rise time and curing time of polyurethane foams and the filler load. This exponential relationship in this study is in complete agreement with the work of another researcher titled "effect of animal waste as filler in flexible polyurethane foam" [8].

Density

Foam density is a specific measurement of how much weight in kilograms polyurethane foam can handle per cubic meter.

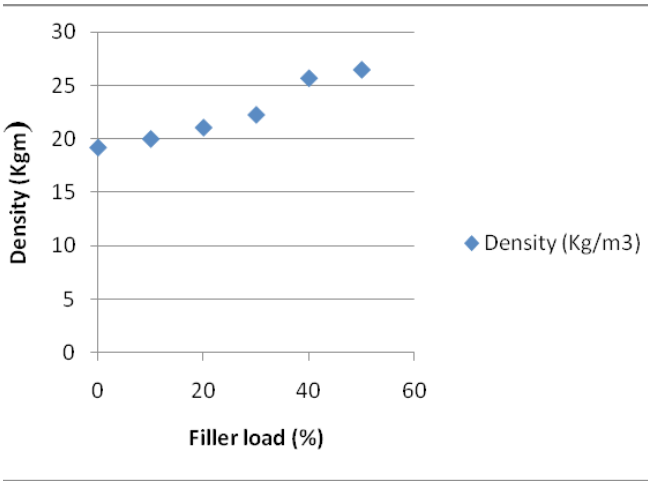

Figure 1. Effect of filler load on Density.

It was observed from the results that as the filler load increased the density of the foam samples also increased. A density of 22.00 was set for the calculations involved in this foam formulation. This could be attributed to the nature and high content of the fillers which would fill up more voids, thus increasing the foam's density [14]. The filled voids tend to make the polyurethane foam structures more compact hence increasing its weight and making it denser.

In flexible polyurethane foams, the fillers promote an increase in density and hence increase the shelf life and cushioning effect of the foam [3]. The same trend was observed in the following works [11,14-16].

Compression Set

The compression set test results were obtained by finding the difference between the initial weight of the foam sample before and after compression.

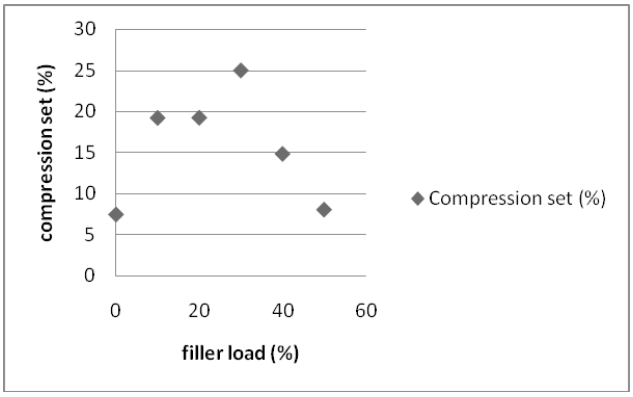

Figure 2. Effect of filler loading on compression set of flexible polyether foam

It was observed that as the filler load increased, the compression strength of the foam also increased as seen in Figure 2. However there was a sharp decline in compression strength in samples 5 and 6. This showed that the presence of the filler improved the ability of the foam to return to its normal shape after compression. This could be due to the reinforcing property of the filler as a result of its cellulosic nature. The sharp decline in compression strength of samples 5 and 6 could be attributed to the fact that though sample 5 and 6 with filler load 40% and 50% respectively have the highest density, they still had the lowest ability to return to their original size after compression. This implies that there is no direct relationship between compression and the density of a foam sample [8]. From the result, it can also be seen that the highest value for the compression set test (25%) was obtained from sample 4 with a filler load of 30%. This shows that the maximum yield for this combination of filler (periwinkle and African star seed shell) for compression set test is obtained when the sample contains 30% of the filler. These findings are in agreement with the works of some other researchers [8,11].

Tensile Strength

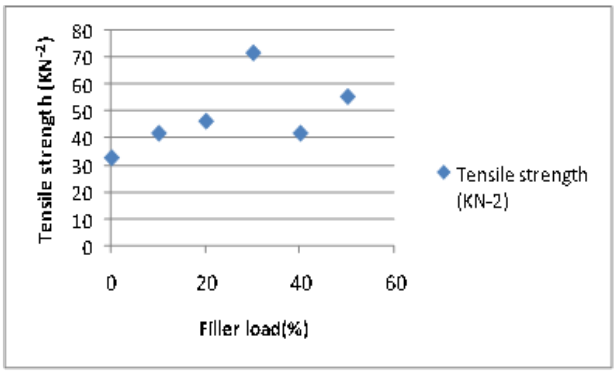

Figure 3. Effect of filler loading on tensile strength of flexible polyether foam

It was seen that the tensile strength of the periwinkle and African star seed shell filled polyurethane foam increased as the filler load increased, but there was a sharp decline in tensile strength in sample 4 and an increase in sample 5 as shown in Figure 3. The increase in tensile strength can be attributed to good interaction between filler- polymer matrix. It could also be due to nature and small particle size of the filler thereby by providing a good surface area to resist stress. Hence, this proves that the filler is suitable and can be applied in the production of polyurethane foams since it improved the mechanical properties of the foam [17]. However, the sharp decline in the tensile strength of the foam sample 4, could be attributed to poor filler interaction between the filler and polyurethane matrix. It could also be attributed to the

voids created by the fillers in the matrix phase [18]. From the results, it can also be inferred that the optimum yield for the tensile strength test is obtained when the sample contains 30% of the filler load, as sample 4 has the highest value (71.7) from the experiment. The rise and fall in tensile strength in the property of this work [10].

Elongation at Break

The results were obtained from a power accurate grip Indentiometer, which recorded elongation as the distance moved by the sample before break.

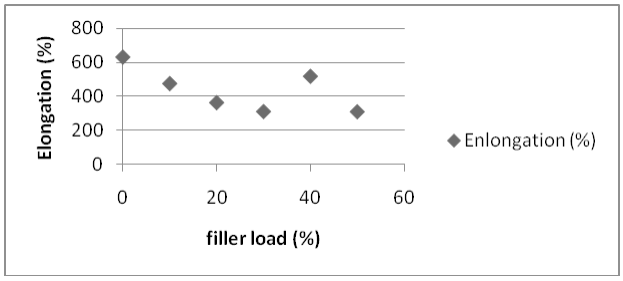

Figure 4. Effect of filler load on Elongation at break

From Figure 4, it is shown that as the filler load increased, there was a corresponding decrease in the elongation at break of the polyurethane foam samples. This inverse relation can be attributed to the nature of the filler (cellulosic) which makes the foam sample tend to elongate more with a lesser filler load than a higher one [19]. Comparing the control (sample1) with the other samples, it is observed from the results that there is an overall decrease in the % elongation at break. However, in sample 5 which has a filler load of 40%, the highest value is obtained (518.55) which although lesser than the control (indicating that there is a decrease) is still much higher in value than the sample containing 10%, 20%, 30% and 50% filler load. Hence it can be inferred from the experiment that the maximum load carrying capacity is obtained when the sample contains 40% of the filler. This trend of results has also been observed in works [16,20].

Flammability Test

The flammability of a polyurethane foam sample is dependent on the amount of oxygen available and the nature of the filler incorporated into the foam [16].

It is observed that as the filler load increased, the flammability of the foam sample decreased, as seen in Figure 5. This can be attributed to the fact that as the filler load increases, it reduces the size of the cell window in the foam structure, hereby hindering the easy passage of oxygen through the foam structure and thus, reducing the flammability of the foam. Since polyurethane products especially foams play a vital and indispensable role in everyday life because of their wide range of application in automobile, household, refrigerators, insulators, reducing the fire risk of such products is very essential [21]. Hence, the addition of biodegradable fillers such as periwinkle and African star seed shells are highly advantageous as they help to reduce the flammability of polyurethane foam. This trend of results was also obtained in the work [22].

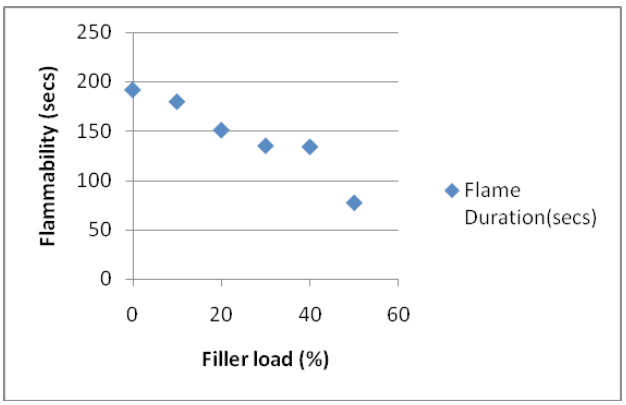

Figure 5. Effect of filler load on flammability.

Hardness test (Indentation hardness)

The firmness of the polyurethane foam is as a result of a measure of the physical property called the indentation force deflection (IFD).

Table 3. Results for the indentation force deflection (IFD) or hardness test.

S/N	samples	Filler load(%)	25%	40%	60%
1	S_1	0	106.20	129.00	269.20
2	S_2	10	119.50	142.00	270.00
3	S_3	20	120.00	149.00	280.20
4	S_4	30	135.00	202.00	300.00
5	S_5	40	139.00	210.00	320.00
6	S_6	50	142.00	240.00	360.00

From Table 3, it was observed that as the filler load increased, the hardness of the foam also increased. This implies that increase in filler load has a positive impact on the hardness of the polyurethane foam material. The fillers exhibited hard effect on the foam and would carry a lot of weight over a long period of time without collapsing immediately. These filler materials are lingo-cellulosic materials and have been proven to be very strong and durable [18]. Furthermore, the 65% IFD exhibited the highest hardness and this could be due to the nature and particle size of the fillers as well as the interaction between the polymer matrix- filler phase. 25% and 40% showed values less than 65% though the increase in hardness was

displayed. The filler added in foam formulation modify the foam's hardness, improving the dimensional stability. Hence the increase in filler load increases the load bearing properties of the foam sample. This trend of results was also obtained in works [10,23].

Surface morphology

The surface morphology of the polyurethane foam which is a function of the filler-foam interaction was observed using a scanning electron microscope.

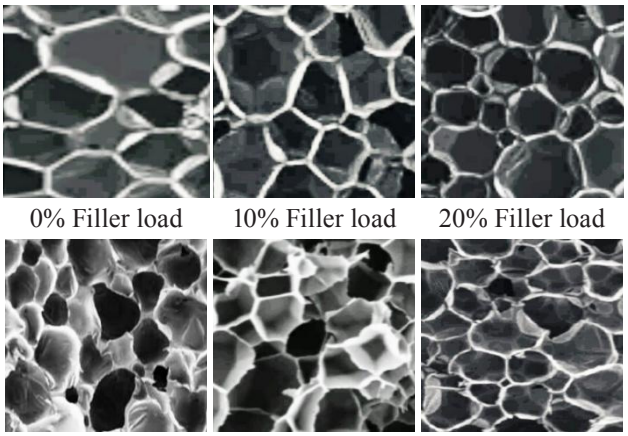

0% Filler load 10% Filler load 20% Filler load

30% Filler load 40% Filler load 50% Filler load

References

[1] Mills, J.N. (2007): Polyurethane Foam: Processing and Microstructure; Polymer Foams handbook, pp.19- 37.

[2] Oertel, G. and Abele, L. (1985): Polyurethane Handbook: Chemistry, Raw Materials, Processing, Application, Properties; Hanser Publishers, Distributed in USA by Scientific and Technical Books, Macmillan. Pp.1- 25.

[3] Billmeyer, F.W. (2005): Textbook of Polymer Science, 3rd edition, John wiley and sons, Toronto, p.447.

[4] Udhayasankar, R., Karthikeyan, B. (2015): A Review on Coconut Shell Reinforced Composites; *International Journal of Chemistry And Technology Research,*8(11):624-637.

[5] Onuegbu T.U., Obi J.N., Ejikeme C. (2010): The Effects of Palm kernel Powder as Filler in Flexible Polyether Foam; *Journal of Physical Sciences, Ghana,*2(4): 126-129.

[6] Babalola, F.U. and Dominic, E.(2012): A Comparative Ananlysis of the Effects of Calcium Carbonate and Dolomite as Fillers in Polyurethane Foam Product. *Journal of Innovations in Science and Engineering,*34-40.

[7] Raju G.U., Kumarappa S., Gaitonde V.N (2012): Mechanical and Physical Characterization of Agricultural Waste Reinforced Polymer Composites; *Journal of Material and Environmental Sciences*,3(5): 907- 916.

[8] Onuegbu T.U., Obianuko, N., Mbachu, G.U., and Iloamaeke, I.M., (2010), Effect of Animal Waste (Goat Femur) As Filler in Flexible Polyether Foam, *Journal of Basic Physical Research,* Vol 1(1):5-8.

[9] Toro P, Quijad R, Yazdani- Pedram M, and Arias J.L. (2007), Eggshell, a new bio-filler for polypropylene composites, Materials Letters, Vol. 61(22): 4347-4350.

[10] Chris-Okafor, P.U., Arinze, R. U., Nwokoye, J.N. and Umar, E. U. (2017); Effects of Coconut Husk and Corn Cob as Fillers in Flexible Polyurethane Foam. *American Journal of Polymer Technology* 3(4):64-69.

[11] Chris-Okafor, P.U., Arinze, R.U., Ekpunobi, U.E., and Anugwom, M.C. (2017); Effects of Mixed Rice Husk and Corn Cob as Fillers on Some Properties of Flexible Polyether Foam. *Global Journal of Science Frontier Research:* B Chemistry 17(2): 30-37.

[12] Manjunatha, G.H. andSabeel, A.K. (2017) : Experimental Characterization of Coconut Shell Particle Reinforced Epoxy Composites; *Journal of Materials and Environmental Sciences,*8(5): 1661- 1667.

[13] Nigerian Industrial Standard 53(1979): Method of Polyurethane Production.

[14] Saliba, C.C., Oréfice, R.L., Carneiro, J.R.G., Duarte, A.K, Schneider, W.T. and Fernandes, M.R.F. (2005); Effect of the incorporation of a novel natural inorganic short fiber on the properties of polyurethane composites. *Polymer Test.;* 24(7): 819-824.

[15] Samuel, E.A. , Ganiyu, K. L., Tinuade J. A. , Semiu A. K., (2015); Model Predictive Performance of Filled Flexible Polyurethane Foam. *American Journal of Polymer Science;* 5(1): 1-9.

[16] Onuegbu, T.U., Ugwu, I.E., Ogunfeyitimi, O. (2013): Physico- mechanical Properties of Flexible Polyether foam: Comparative Effects Of Fillers; *Chemistry And Materials Research,* 3:46-52.

[17] Dalen, M.B., Ibrahim, A.Q., Adamu, H.M., and Nurudeen, A.A., (2014), Effect of calcium carbonate and kaolin filler loading on curing rates of polyurethane foams, International research *Journal of pure and applied chemistry;* Vol. 4(6):691-694.

[18] Ruijun, G., Mohim, M.S. and Samir, K.K. (2013): A Feasible Study of Polyurethane Composites Foam with Added Hardwood Pulp, Industrial Crops and Products; *Checkmate Press, New York,*42(2):273-279.

[19] Javni, I., Song, K., Lin, J., Petrovic, Z. (2011): Struc-

ture and Properties of Flexible Polyurethane Foams with Nano- and Micro- Fillers;*Journal of Cellular Plastics,*47(4):357-372.

[20] Agarry, S.E., Latinwo, G.K.,Afolabi,T.J., Kareen, A.S. (2015): Model Predictive Performance of Filled Flexible Polyurethane Foam; *American Journal of Polymer Science,* 5(1):1-9.

[21] Gharenbagh, A. and Ahmadi, Z. (2012): Polyurethane Flexible Foam Fire Behaviour, INTECH Open Access Publisher, Pp.1-10.

[22] Sant'Anna, S.S., Souza, D.A, Carvalho, C.F. and Yoshida, M.I. (2008): Morphological and Thermal Analyses of Flexible Polyurethane Foams Containing Commercial Calcium Carbonate; Ecletica, 33(2): 55-60.

[23] Agham, R.D. (2013): Performance of Coconut Husk Mixed Polyurethane Foam as an Alternative Insulating Material; *International Journal of Engineering and Innovative Technology,* 9(2): 100-104.

BILINGUAL PUBLISHING CO.
Pioneer of Global Academics Since 1984

Organic Polymer Material Research
https://ojs.bilpublishing.com/index.php/opmr

ARTICLE

Thermo-oxidative Oligomerization of Aromatic Diamine

B. A. Zaitsev* L. G. Kleptsova I. D. Shvabskaya A.E. Bursian

Institute of Macromolecular Compounds, Russian Academy of Sciences, Saint Petersburg, 199004, Russia

ARTICLE INFO

Article history
Received: 23 August 2021
Accepted: 15 September 2021
Published Online: 15 October 2021

Keywords:
Aromatic diamines
Oxidative oligomerization
Thermal properties
Molecular spectroscopy

ABSTRACT

Molecular spectroscopy (electronic, FT-IR, NMR), methods of thermal and elemental analysis were used for the first time to describe the process of thermo-oxidative oligomerization of 1,3-bis-(4-aminophenoxy)benzene. Introduction of this monomer into linear and network copolymers makes it possible to improve processability, mechanical strength and heat resistance of materials. The structures of copolymers obtained by thermo-oxidation of the diamine in various thermal regimes were studied. It was demonstrated that during prolonged heating of this diamine in air in the temperature range from 220 to 320°C, oligomeric aromatic diamines were formed; these products contained fragments of benzenoid and quinoid types.

1. Introduction

Aromatic diamines (ADA) find wide application in organic and polymer chemistry, for example, in polyimide synthesis [1-4], as crosslinking additives (curing agents for epoxy resins) [5-7], for polymer stabilization [8]. 1,3-Bis-(4-aminophenoxy)benzene (BAPB) is of special interest. Introduction of units of this diamine into linear and network copolymers considerably improves their useful properties (processability, strength and heat resistance) [9-13]. Our recent publications [14-16] reported preparation of novel network copolymers by high temperature (160-320°C) co-curing of rolivsans (thermosetting polyester-based composites) and aromatic diamines (ADA) in air. These products demonstrated good adhesive properties, high temperature strength and prolonged thermo-oxidative stability at 260-350°C as compared to those of the initial (non-modified) rolivsans (ROL). It was suggested to use BAPB as a comonomer or modifying agent in order to impart lower rigidity, higher temperature strength, and higher thermo-oxidative stability to cured ROL. It was established that co-curing of rolivsans with ADA in air in the temperature interval from 160 to 300 (320)°C involved a set of consecutive-parallel reactions. In the course of these reactions, additional poly(amide) networks were formed as a result of chemical interactions between carboxyl (anhydride) groups (which appeared during thermal transformations of ROL) and amino groups of ADA [17]. However, it was still unclear whether the presence of ADA in the cured ROL-ADA system led only

**Corresponding Author:*
B. A. Zaitsev,
Institute of Macromolecular Compounds, Russian Academy of Sciences, Saint Petersburg, 199004, Russia;
Email: zaitsev@hq.macro.ru

DOI: https://doi.org/10.30564/opmr.v3i1.3612

to the above-mentioned interactions, or other thermo-oxidative transformations of aromatic diamines were possible in this temperature range. In the present work, ROL was not included in the studied system, since it undergoes various chemical transformations in air and thus renders it difficult to investigate reactions of aromatic diamines. It is well known that aromatic diamines form oligomeric polyaniline-like products in the presence of various oxidants [18-20].

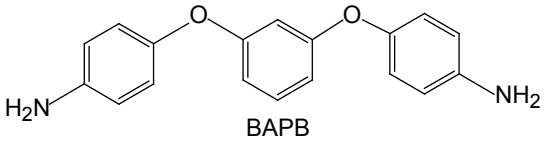

BAPB

The aim of this work was to study chemical structures, compositions and some properties of the products of high-temperature oxidation of aromatic diamines using BAPB as an example.

2. Materials and Method

1,3-Bis-(4-aminophenoxy)benzene (BAPB, 98%, m.p. = 115-118°C) was purchased from TCI America (Portland, USA) and used as received; before obtaining electronic spectra, BAPB was additionally purified by recrystallization from ethanol (m.p. = 117-118°C).

Thermal treatment of BAPB monomer was carried out in siliconized brass mold 30×25 mm in size in air thermostat. The samples were melted down at 120–122°C (the thickness of melt layer was ~2 mm) and heated stepwise for 1 h until the predefined final temperature (T_{fin}) was reached. The following initial (monomeric) and thermally treated diamine samples were obtained under different heating conditions: 1(*20°*), 2(*20°-125°*), 3(*20°-150°*), 4(*20°-160°*), 5(*20-170*), 6*(125°-180°*), 7*(150°-180°*), 8(*125°-200°*), 9(*125°-220°*), 10(*150°-220°*), 11(*125°-240°*), 12(*125°-260°*), 13(*150°-260°*), 14(*125°-280°*), 15(*125°-300°*), 16(*125°-320°*), 17(*150°-350°*), 18(*170°-320°*), 19(*150°-260°/2h,260/20h)*, 20(*150°-260°/2h*, *260/40h)*. The time of temperature rise between steps was approximately 15 min.

For obtaining electronic spectra, samples of the initial (1) and thermally treated BAPB (2-6, 8, 9, 11, 12) in the form of thin powder were treated with chloroform ($CHCl_3$) at room temperature for approximately 24 h. The resulting solutions (extracts) were filtered to remove the precipitate; chloroform was evaporated, and the residue was dried until constant weight was reached (80-85 wt.% of the initial sample mass). These extracts were used to prepare diluted solutions of required concentrations in ethanol and chloroform. Electronic spectra of samples were registered in quartz cuvettes 1 cm wide at room temperature using an SF-256 spectrophotometer (LOMO PHOTONICA, Russia) in the wavelength range of 250–900 nm.

FT-IR spectra of monomeric and thermally treated BAPB in the form of thin powder were taken using a Vertex 70 FT-IR spectrometer (Bruker, Germany) (4000 – 600 cm^{-1}) equipped with an attenuated total reflectance (ATR) attachment (Pike). The FT-IR ATR spectrum of monomeric BAPB (sample 1) included the following absorption bands (cm^{-1}): 3425 and 3406 (symmetric and antisymmetric vibrations of hydrogen atoms in NH_2 groups [18]), 3339 and 3213 (hydrogen bonds involving nitrogen and oxygen atoms), 3082, 3040, and 3013 (valence vibrations of C-H aromatic rings [21]) and 1607 (C_{Ar}), 1582 (C_{Ar} and deformation vibrations of NH_2 [21]), 1503 (C_{Ar}), 1479 (C_{Ar}), 1462, 1312 (C_{Ar}-N), 1269 (valence vibrations of C_{Ar}-N [21]), 1204 (-O- in C_{Ar}-O-C_{Ar}), 1159 (C-O-C), 833 (=C-H). The spectrum of thermally treated BAPB (sample 18) included the bands similar to those of monomer (sample 1). However, the following absorption bands were wide (diffuse) in comparison to those in the monomer spectrum, and had different intensities (cm^{-1}): 3490-3406 (the maximum at 3410), 3400-3300 (the maximum at 3340), 3221-3211 [the maximum at 3213 (valence vibrations of –NH-)], 1589 (C_{Ar}), 1503 (C_{Ar}), 1474 (the benzenoid-type unit [22]), 1447, 1312, 1269 (C_{Ar}-N [21]), 1254 (the benzenoid-type unit C-N [22]), 1204, 1167 (C_{Ar}-O), 1119 (C_{Ar}-O), 1080, 1011, 1003, 964, 831, 770, 683.

The ^{1}H NMR spectra of monomeric and thermally treated diamines were obtained with the use of a Bruker Avance instrument (400 MHz) in deuterated chloroform ($CDCl_3$). Solid state ^{13}C NMR spectra of powdered samples were registered with the use of a Bruker Avance spectrometer (400 MHz) [operating frequency 125.77 MHz, CP MAS (10 kHz)]. The spectra of the initial BAPB (sample 1) contained peaks with the following chemical shifts (δ, ppm). ^{1}H NMR: 7.28-6.57 ($12H_{Ar}$), 3.54 ($4H_N$ for two NH_2 groups); ^{13}C NMR: 209.8, 202.9, 161.7, 159.9, 147.0 (148.4 for aniline [23]), 144.2, 130.4 (129.5 for aniline [23]), 123.3, 122.4, 117.6, 114.8 (115.0 for aniline [23]), 106.6, 103.7, 43.9.

The spectra of thermally treated sample (18) contained peaks with the following chemical shifts (δ, ppm). ^{1}H NMR: 7.28-6.57 (Ar-H), 3.60 (NH_2). ^{13}C NMR: 210.8, 202.6, 161.6, 156.4 (C_{Ar}) 145.7 ($C_{p\text{-}Ar\text{–}N}$) (142.4-146.4 for polyaniline units [24, 25]), 131.1, 130.4, 122.9 (C_{Ar} at 121.7-124.4 for polyaniline [24,25]), 116.4 (116.7-124.4 for polyaniline units [24,25]), 111.9, 82.0, 65.7, 51.3, 42.7, 37.2.

Elemental analysis of sample 1. Found (%): C 73.95, H 5.97, N 9.64; for $C_{18}H_{16}N_2O_2$: calculated (%) C 73.90, H 5.47, N 9.58. Elemental analysis of sample 18: found (%) C 74.29, H 5.47, N 9.60.

Dynamic thermogravimetric analysis (DTGA) of sample 1 was carried out using a Paulik-Paulik-Erdei "Derivatograph C" (MOM, Hungary); the heating rate was 10°C/min [26].

3. Results and Discussion

Thermally treated BAPB samples appeared as dark brown or black homogeneous solid melts; their high temperature viscosity increased with increasing T_{fin}. The solid melts were compositions (mixtures) of monomeric BAPB and products of its thermo-oxidative polycondensation (oligo-BAPB) of various compositions; the products demonstrated good adhesive properties. Upon completion of stepwise thermal treatment (up to T_{fin} = 150-240°C) and subsequent cooling down to room temperature, the melts gradually became solid. They retained stickiness for some time (1-2 days) at room temperature, and it was possible to spun threads of these melts. However, they became solid (rigid, brittle) on long storage due to crystallization processes. When BAPB was treated stepwise up to T_{fin} = 300–320°C, the obtained samples (15–20) became infusible and only partially dissolved in chloroform.

It is known that BAPB and other aromatic (di)amines oxidize easily in air to form colored products of various structures. For example, aniline enters into reaction with relatively weak oxidants, such as H_2O_2, to give polyaniline containing both dehydrogenated and oxidized units $[(-C_6H_4\text{-}NH\text{-}C_6H_4\text{-}NH)/(C_6H_4\text{-}N{=}C_6H_4{=}N)]_n{\sim}$ [27]. Strong oxidizing agents not only transform NH_2 fragment to NO_2, but also attack activated aromatic rings, which results in formation of numerous products [28].

In the process of high temperature treatment of BAPB up to T_{fin} = 320°C (sample 18), solid black infusible product was formed; elemental analysis revealed that nitrogen and carbon contents in this substance virtually coincided with those of the initial monomer (sample 1). This temperature regime did not cause noticeable thermo-oxidative destruction of the diamine, which was also confirmed by the data of thermal analysis.

According to the data of thermal analysis (DTGA and DTA) [26], fast heating of sample 1 in air (on thermobalance) in the temperature range from 20 to 400°C leads not only to its thermo-oxidative polycondensation with formation of oligomers (oligo-BAPB), but also to sublimation (~20%). Sublimation rate reaches its maximum at ~ 400°C. At temperatures exceeding 450°C, intensive thermo-oxidative destruction of the sample was observed. Upon heating of infusible samples 19 and 20 (obtained by thermal treatment of BAPB with exposure at T_{fin} = 260°C for 20 and 40 h, respectively), the values of mass loss attributed to sublimation were equal to 15.75% and 16.33%, respectively. Similar sublimation process occurred during prolonged exposure of sample 18 at 350°C (Figure 1).

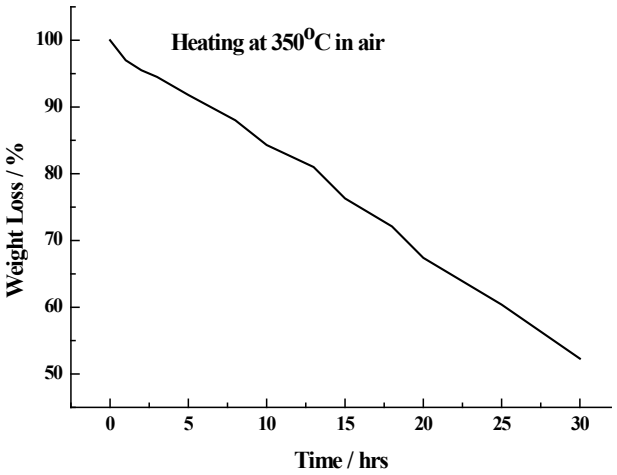

Figure 1. Dependence of mass loss of sample 18 obtained by stepwise heating of BAPB monomer (sample 1) to T_{fin} = 320°C on the time of air exposure at 350°C.

Thermal oxidation of BAPB was studied by molecular spectroscopy. Elemental analysis of thermally treated samples and analysis of their ^{1}H NMR spectra (Table 1, Figure 2) showed that oxidative oligomerization of BAPB samples did not lead to substantial changes in their chemical compositions.

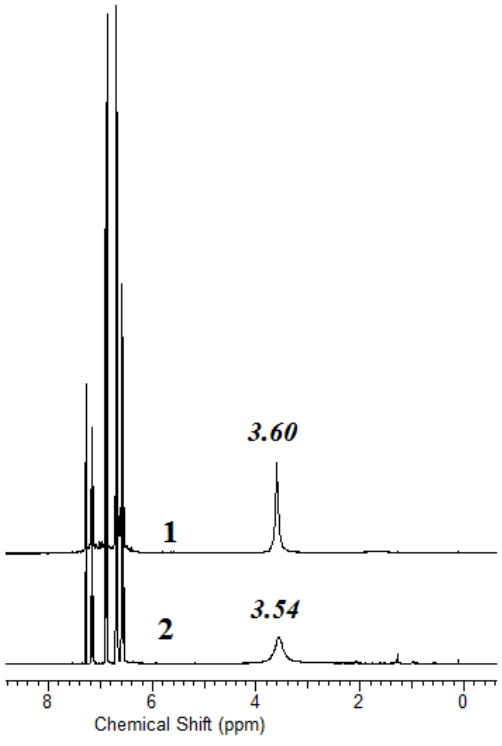

Figure 2. ^{1}H NMR spectra of thermally treated (sample 18) and initial (sample 1) BAPB

Table 1. Dependence of hydrogen content in BAPB samples on heating regime in air according to the data of ^{1}H NMR spectroscopy

Sample	T_{fin} [a], °C	$\Sigma H_N/\Sigma H_{Ar}$ [b]	$\Sigma H_N/\Sigma H_j$ [c]	Elemental analysis, %		
				C	N	H
1	20	0.32	0.24	73.94	9.64	6.15
2	125	0.32	0.24	-	-	-
3	150	0.32	0.24	-	-	-
4	160	0.32	0.24	-	-	-
5	170	0.32	0.23	-	-	-
6	180	0.31	0.23	74.04	9.60	5.80
7	180	0.31	0.23	-	-	-
8	200	0.31	0.23	-	-	-
9	220	0.31	0.23	74.04	9.54	5.75
10	240	0.30	0.22	-	-	-
11	260	0.30	0.21	74.24	9.62	5.68
20	260[d]	0.25	0.17	71.30	9.27	5.55
14	280	0.27	0.21	-	-	-
15	300	0.27	0.20	74.23	9.50	5.62
16	320	0.27	0.20	74.20	9.57	5.53
18	320	0.28	0.21	74.24	9.60	5.37

[a] T_{fin} is the final temperature of thermal treatment.

[b] ΣH_N and ΣH_{Ar} are the integral intensities of proton signals of amino groups (d = 3.57 ±0.03 ppm) and aromatic rings (d = 6.5-7.3 ppm), respectively.

[c] ΣH_N and ΣH_j are the integral intensities of all proton signals.

[d] The sample was exposed at 260°C for 40 h in air.

The values of hydrogen content in heated samples decreased insignificantly with increase in BAPB heat treatment temperature from 260 to 320°C, since its thermo-oxidative (poly)condensation in air was accompanied by liberation of water (Figure 3):

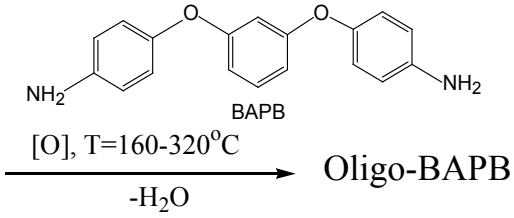

Figure 3. Thermo-oxidative (poly)condensation of BAPB

These first data on the products of thermo-oxidation (oligo-BAPB) obtained in the above-mentioned specific temperature-time regimes raised some questions about composition and chemical structure of oligo-BAPB. It is possible that these oligomers are similar to the well-studied initial products of oxidation of aromatic mono- and diamines (e.g., low molecular weight polyanilines $[(-C_6H_4-NH-C_6H_4-NH)/(C_6H_4-N=C_6H_4=N)]_n$~[27]), although polyanilines are obtained under entirely different conditions. BAPB contains two symmetrically arranged sites that possess equal oxidation abilities. The oxidation reaction yields dimers, soluble branched structures, and infusible (insoluble, crosslinked) products (samples 15–20). Thus, it can be concluded that depending on temperature-time regime (which can be harsh or mild), oxidation may involve both one and two sites.

However, upon prolonged (40 h) exposure of sample 20 at 260°C (Table 1), contents of hydrogen, nitrogen and carbon decreased significantly, which indicated deeper thermo-oxidation processes.

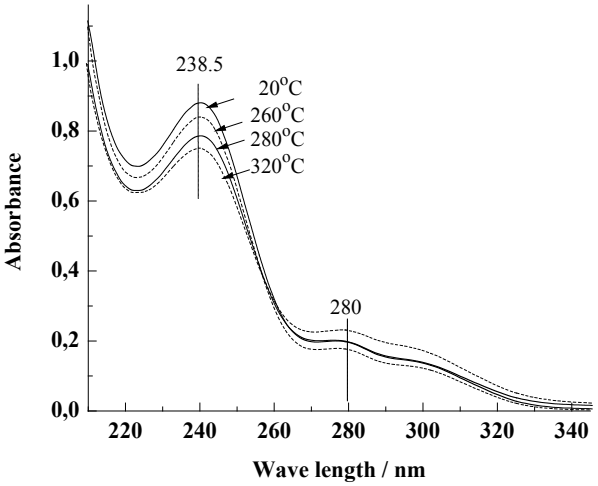

Figure 4. UV spectra of ethanol solutions (c = ~10^{-5} g/mL) of BAPB samples (1, 20, 14, 16) treated according to stepwise regime with various final temperatures T_{fin} (°C): 20, 260, 280 and 320, respectively.

As is seen in Figure 4, UV spectra of ethanol-soluble BAPB samples include intense absorption bands at ~240 and 280 nm, which are typical of (poly)aniline and polymers of other (amino)substituted benzene derivatives [29,30]. Since it is the initial diamine that mainly dissolves in ethanol, under harsh conditions of thermo-oxidative condensation its contents in samples naturally decreases. Therefore, the intensity of absorption band at 238.5 nm also decreases.

Electronic spectra of chloroform extracts (solutions) obtained from thermally treated BAPB samples (Figure 5) contain wide absorption bands in the 340-800 nm region; intensities of these bands increase significantly upon increase in the final temperature (T_{fin}) from 220 to 320°C. The bands at 475, 510 and 580 nm become more pronounced. Since elemental composition of oligomerized samples differs only slightly from that of the initial (monomeric) BAPB (Table 1, samples 5-6), it is believed that the above-mentioned samples virtually do not contain products of deep oxidation. This observation simplifies the problem of composition and chemical structure of oligo-BAPB. Processes of oxidation of its structural analogs (aniline and some aromatic diamines) are well studied, which facilitates comparative analysis. For example, electronic absorption spectra of aniline dimer (N,N′-diphenyl-1,4-phenylenediamine) [31] and N,N′-bis (4'-amino-phenyl)-1,4-quinone diimine [32] (which are used in our work as model compounds) contain wide maximums in the long-wavelength region. These peaks (475 and 575 nm [31] and 550-629 nm [32]) are attributed to benzenoid and quinoid fragments; at the same time, the spectrum of N,N′-bis(4'-aminophenyl)-1,4-quinone diimine includes the peak at λ_{max}=572 nm [33]. Comparison of electronic spectra of our samples (Figure 4) and the spectra of model compounds and low molecular weight aniline also suggests that these compounds are structurally similar. Moreover, it is expected that, unlike benzenoid structures, conjugated quinoid fragments should give more intensive long-wavelength peaks with higher bathochromic shifts. It is also seen in Figure 5 that the intensity of the band located in the 580-800 nm area is significantly lower than those of the bands observed in the short-wavelength region (350-475 nm), the concentrations of oligo-BAPB being almost equal. These results (together with the data of elemental analysis and ^{1}H NMR spectroscopy) indicate that oligo-BAPB samples contain both quinoid and benzenoid fragments, the latter predominating.

Since thermally treated samples are mixtures of monomeric BAPB and oligo-BAPB, their FT-IR spectra contain the absorption bands typical of each related compounds, although with different intensities. The spectrum of thermally treated BAPB (sample 18) includes the same absorption bands as that of the monomer (1), but they are diffuse and have lower intensities. Thus, intensities of the Ar band (1607 cm^{-1}) and the bands attributed to terminal amino groups (1312, 1269, 1092, 1009, 746 cm^{-1}) in the spectra of thermally treated samples decrease sharply in comparison to those in the spectrum of monomeric BAPB. A new band (1254 cm^{-1}) typical of C–N group near benzenoid ring appears [22,34]. As seen in Figure 7, ^{13}C NMR spectrum of insoluble and infusible

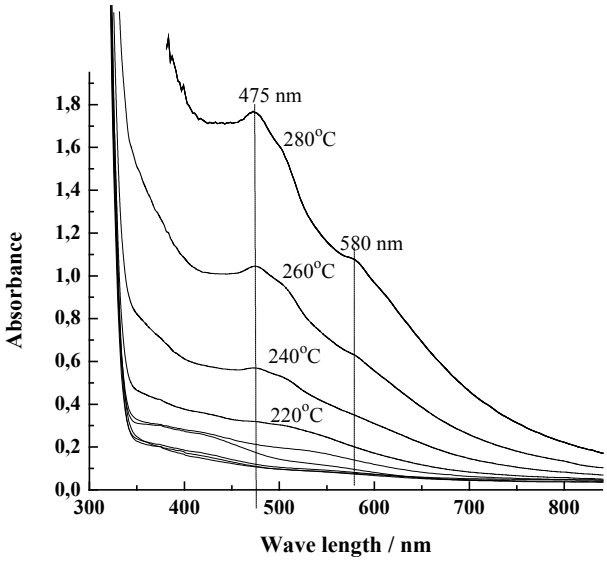

Figure 5. Electronic absorption spectra of chloroform solutions (c = ~10^{-3} g/mL) of thermally treated BAPB samples; the samples were obtained by stepwise heating of BAPB up to final temperatures indicated in the spectra. λ is the wavelength (nm).

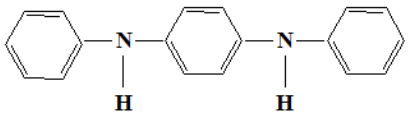

(N,N'-diphenyl-1,4-phenylenediamine)

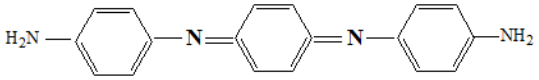

(N,N'-bis(4'-aminophenyl)-1,4-quinonediimine)

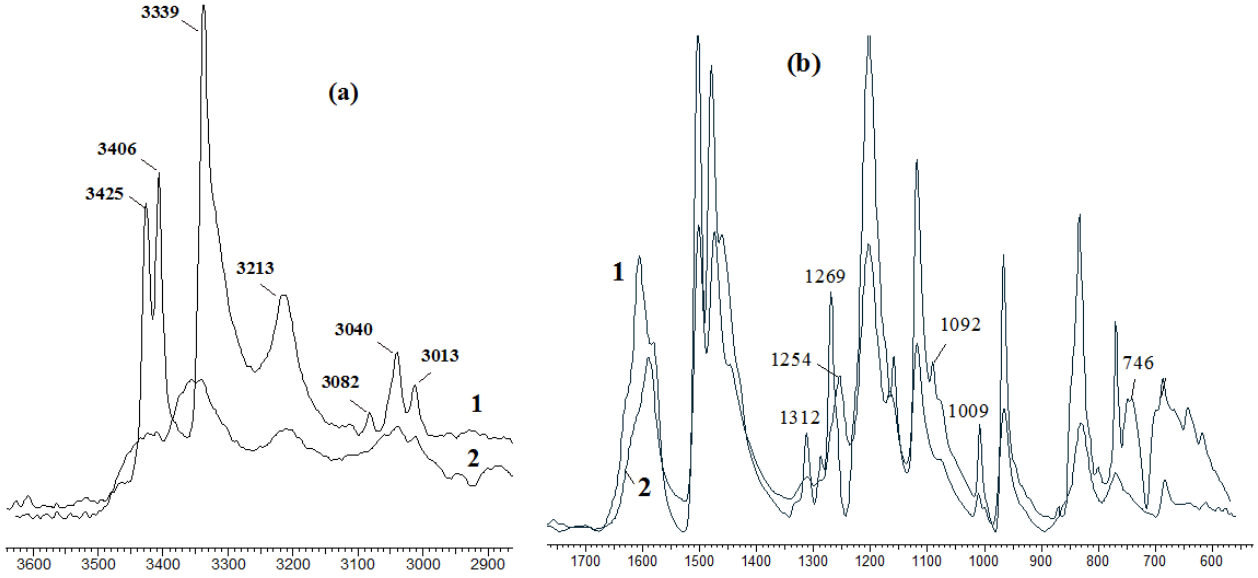

Figure 6. FT-IR spectra of monomeric (1) and thermally treated BAPB (2, sample 18)(Wavenumber, $cm^{-1)}$

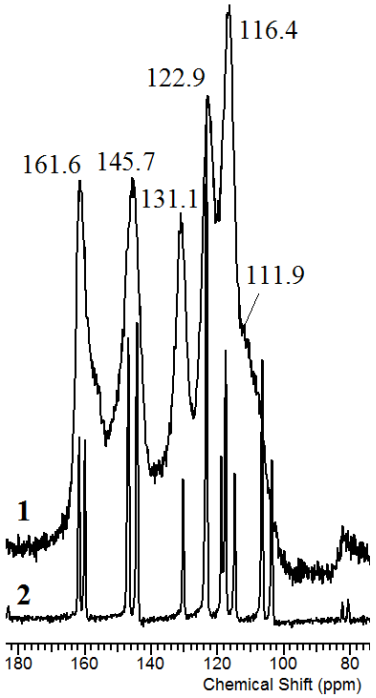

Figure 7. ^{13}C NMR spectra of thermally treated sample 18 (1) and the initial BAPB sample 1 (2).

sample 18 is poorly resolved. However, it can be noted that resonance peaks of protonated carbon atoms at 156.4 (C_{Ar}), 145.7 ($C_{para\text{-}Ar\text{-}N}$), 131.1, 130.4, 122.9, and 116.4 ppm are related both to benzenoid and quinoid fragments [21,22]; the peak at 116.4 ppm (benzenoid rings) has the highest intensity.

4. Conclusions

Using 1,3-bis-(4-aminophenoxy)benzene (aromatic diamine applied in preparation of various heat-resistant polymers, polymer materials and composites) as an example, the process of thermo-oxidation of aromatic diamines by air oxygen was investigated. It was revealed that during heating in air up to ~200-220°C this diamine retained its chemical stability, and at higher temperatures (260-320°C) it underwent oxidative (poly)condensation accompanied by release of water.

It was demonstrated that oligomeric products of thermo-oxidation were mixtures of 1,3-bis-(4-aminophenoxy)benzene and its dimers, soluble linear and branched oligomers, and crosslinked (insoluble) polymers; they retained chemical stability during heating in air at 350°C for several tens of hours. Using molecular spectroscopy methods, elemental and thermal analysis, it was established that the obtained oligomers contained fragments of benzenoid and quinoid types. The obtained results are of practical importance, since they reveal thermo-oxidative transformations of aromatic diamines that are possible in the temperature range from 170 to 350°C. These temperatures are relevant for preparation and operation of thermosetting polyimides, epoxides and other materials (e.g., rolivsans modified with aromatic diamines).

Acknowledgements

The authors are grateful to E.N.Vlasova and E.V.Parilova (research workers of Laboratory of polymer spectroscopy of IMC RAS) for obtaining FT-IR, ^{1}H and ^{13}C NMR spectra.

Conflict of Interests

The authors have no conflicts of interests to declare.

Author Contributions

Zaitsev Boris A.: formulation of the problem; general direction, analysis and interpretation of the results obtained by molecular spectroscopy and thermal analysis.

Kleptsova Larisa G.: synthesis, studies of thermal properties of the obtained monomer-oligomer compositions.

Shvabskaya Irina D.: preparation of samples for FT-IR and NMR spectroscopy and analysis of the obtained results.

Bursian Anna E.: electronic spectroscopy of solutions of samples of various compositions (at constant concentration) and comparative analysis of the obtained results.

References

[1] *Ghosh M.K., Mittal K.L.* Polyimides Fundamentals and Applications. New York: Marcel Dekker Inc., 1996. 891P.

[2] High Performance Polymers—Polyimides Based—From Chemistry to Applications (ed. *M. J. M. Abadie*). Rijeka.: InTech, 2012. 244 P. https://doi.org/10.5772/2834.

[3] Handbook of composites /ed. *G. Lubin*. New York. etc.: Van Nostrand Reinhold Co, 1982. 786 P. https://doi.org/10.1007/978-1-4615-7139-1.

[4] *Buhler K.U.* Spezialplaste. Berlin: Akademie-Verlag, 1978.

[5] Chemistry and Technology of Epoxy Resins / ed. *B. Ellis*. Dordrecht: Springer Science+Business Media, 1993. https://doi.org/10.1007/978-94-011-2932-9.

[6] *Siddiqi H.M., Afzal A., Sajid S., Akhter Z.* Synthesis, characterization and thermal oxidative stability of rigid epoxy polymers cured from aromatic mono- and di-amines. // J. Polym. Res. 2013, V.20, N 41. https://doi.org/10.1007/s10965-012-0041-0.

[7] *Förster P., Hauschildt K. R., Wilhelm D.* The effect of different hardeners on the ageing of crosslinked epoxy resins. // Makromol. Chem. Macromol. Symp.,1991,V. 41, N 1, P.141-151.https://doi.org/10.1002/masy.19910410112.

[8] *Pospigil J.* Aromatic and Heterocyclic Amines in Polymer Stabilization In: *POLYMER*, 2005, V. 124, part of Adv. Polym. Sci., P. 87-189.

[9] *Graham, M. J.* Synthesis and characterization of wholly aromatic semicrystalline polyimides based upon bis(4-aminophenoxy) benzenes. PHD Dissertation,-January,1999.Blacksburg,Virginia. P. 156., 185 P.

[10] *Chao M., Kou K.C., Wang Z.C., Wu G.L., Zhang D.N., Zhang J.Q.* Synthesis and characterization of polyimides derived from novel 1, 3-bis (4-aminophenoxy) benzene. // Adv. Mater. Res. 2011, V. 199-200, P. 13-18. https://doi.org/10.4028/www.scientific.net/AMR.199-200.13.

[11] Ratta V., Ayambem A., McGrath J.E., Wilkes G.L. Crystallization and multiple melting behavior of a new semicrystalline polyimide based on 1,3-bis(4-aminophenoxy)benzene (TPER) and 3,3′,4,4′-biphenonetetracarboxylic dianhydride

(BTDA). // Polymer. 2001, V. 42, N14, P. 6173-6186. https://doi.org/10.1016/S0032-3861(01)00010-6.

[12] *Zhang H., Wang W., Chen G., Zhang A., Fang X.* Melt-Processable Semicrystalline Polyimides Based on 1,4-Bis(3,4-dicarboxyphenoxy)benzene Dianhydride (HQDPA). Synthesis, Crystallization, and Melting Behavior. // Polymer. 2017, V. 9, N 9, 420 (P. 1-17). https://doi.org/10.3390/polym9090420.

[13] *Chao M.* Synthesis and Characterization of Semicrystalline Polyimides Containing Bridged Linkages. // Int. J. Polym. Sci. 2018, V. 2018, Article ID 8590567. https://doi.org/10.1155/2018/8590567.

[14] *Zaitsev B. A., Shvabskaya I. D., Kleptsova L.G.* Novel polycondensation method of improving high-temperature properties of microheterogeneous rolivsan copolymers modified by inserting epoxy and imide bridges between spherical microdomains. // High Perform. Polym. 2017, V. 29, P. 636–645. https://doi.org/10.1177/0954008317696564.

[15] *Zaitsev B. A., Shvabskaya I. D., Kleptsova L.G.* High-Temperature transformations of aromatic diamines in the rolivsan matrix. // Russ. J. Appl. Chem., 2017, V. 90, № 6, P. 946−955. https://doi.org/10.1134/S1070427217060179].

[16] *Zaitsev B. A.* Combination of polymerization and polycondensation in the synthesis, chemical modification, and cure of rolivsan thermosetting resins. // High Perform. Polym. 2018, V. 30, P. 211–223. https://doi.org/10.1177/0954008316688760.

[17] *Zaitsev B.A., Kleptova L.G., Shvabskaya I.D.* Studies of formation mechanism, structure and properties of network copolymers obtained by co-curing of rolivsan thermosetting resins with aromatic diamines. // *Int. J. Polym. Sci*. 2019, V. 2019, Article ID 1601236 (P. 1-15). https://doi.org/ 10.1155/2019/1601236.

[18] H.A. Matnishyan, T.L. Hakhnazaryan. Oxidative Polycondensation of Aromatic Amines. *Polymer Science, series A,* 2004, Vol. 46, No. 12, p. 1220-1227.

[19] Mezhuev Y.O., Korshak Yu.V., Shtil'man M. I., Koledenkov A.A. Kinetic model of oxidative polymerization of aniline. *Advances in chemistry and chemical technology* . - 2008. - T. 22, No. 5. - P. 39–43.

[20] A.A. Koledenkov, Ya.O. Mezhuev, D.V. Tkachenko The mechanism of oxidative polymerization of p-phenylenediamine. *Advances in chemistry and chemical technology*. - 2010. - T. 24, No. 4. - P. 44–47.

[21] *Bellamy L.J.* The Infra-Red Spectra of Complex Molecules. 2nd ed. New York: John Wiley & Sons, Inc., 1958.

[22] *Xin-Gui Li, Mei-Rong Huang, Wei Duan, Yu-Liang Yang.* Novel Multifunctional Polymers from Aromatic Diamines by Oxidative Polymerizations. Chem. Revs. 2002, V. 102, N. 9, P. 2925-3030.

[23] Chemical book, Aniline(62-53-3), ^{13}C NMRwww. chemicalbook.com. https://www.chemicalbook.com/chemicalproductproperty_en_cb7169544.htm.

[24] *Ni S., Tang J., Wang F., Shen L.* ^{13}C n.m.r, characterization of soluble polyaniline // Polymer. 1992, V. 33, N.17, P. 3607-3610.

[25] *Hjertberg, T., Salaneck, W. R., Lundstrrm, I., Somasiri, N. L. D., MacDiarmid, A. G.* J. A 13C CP-MAS NMR investigation of polyaniline. // Journal of Polymer Science: Polymer Letters Edition, 1985, V. 23, 503-508. https://doi.org/10.1002/pol.1985.130231002.

[26] *Zaitsev B.A., Kleptsova L.G., Shvabskaya I.D.* Heat-Resistant Network Copolymers Based on Rolivsans Modified with Aromatic Diamines. Russ. J. Appl. Chem. 2017, V. 90, N 3, P. 406−413. https://doi.org/10.1134/S1070427217030132%5d.

[27] *Moon D.K., Osakada K., Maruyama T., Yamamoto T.* Preparation of polyaniline by oxidation of aniline using H_2O_2 in the presence of an iron (I1) catalyst. Makromol. Chem. 1992, V. 193, P. 1723 -1728.

[28] *Nielsen, A.T.* Nitrocarbons. Weinheim: Wiley-VCH. 1995. https://doi.org/10.1002/recl.19961150909.

[29] *Kumar S., Nanak G. Organic Chemistry.* Spectroscopy of Organic Compounds. Amritsar: Dev University, 2006.

[30] *Kapelle S., Rettig W., Lapouyade R.* Aniline dimers and trimers as model compounds for polyaniline. // Chem. Phys. Lett. 2001, V.348, N 5-6, P. 416-424. https://doi.org/10.1016/S0009-2614(01)01139-3.

[31] *Bogomolova O.A., Sergeyev V.G.* Acid Doping of Phenyl-Capped Aniline Dimer: Intermolecular Polaron Formation Mechanism and Its Applicability to Polyaniline. // J. Phys. Chem. A 2018, V. 122, N 2, P. 461–469. https://doi.org/10.1021/acs.jpca.7b09851.

[32] *Gizdavic-Nikolaidis M.R., Zujovic Z.D., Ray S., allan j. Easteal A.J., Bowmaker G.A.* Chemical Synthesis and Characterization of Poly(aniline-co-ethyl 3-aminobenzoate) Copolymers. // J. Polym. Sci., Polym. Chem. Part. A. 2010, V. 48, N 6, P. 1339-1347. https://doi.org/10.1002/pola.23895.

[33] *Gong J., Cui X.-J., Chen Y.-G., Xie Z.-W., Qu L.-Y.* UV-Vis Spectra of N, N '-Bis(4'-Aminophenyl)-1,4-quinonenediimine Doped with H4SiW12O40 // Macromolecular Research 2004. V. 12, N. 1, P. 22-25.

[34] *Gupta K., Jana P. C., Meikap A. K.* Synthesis, electrical transport and optical properties of polyaniline-zirconium nanocomposite. // J. Appl. Phys. 2011, V. 109, P. 123713. https://doi.org/10.1063/1.3597626.

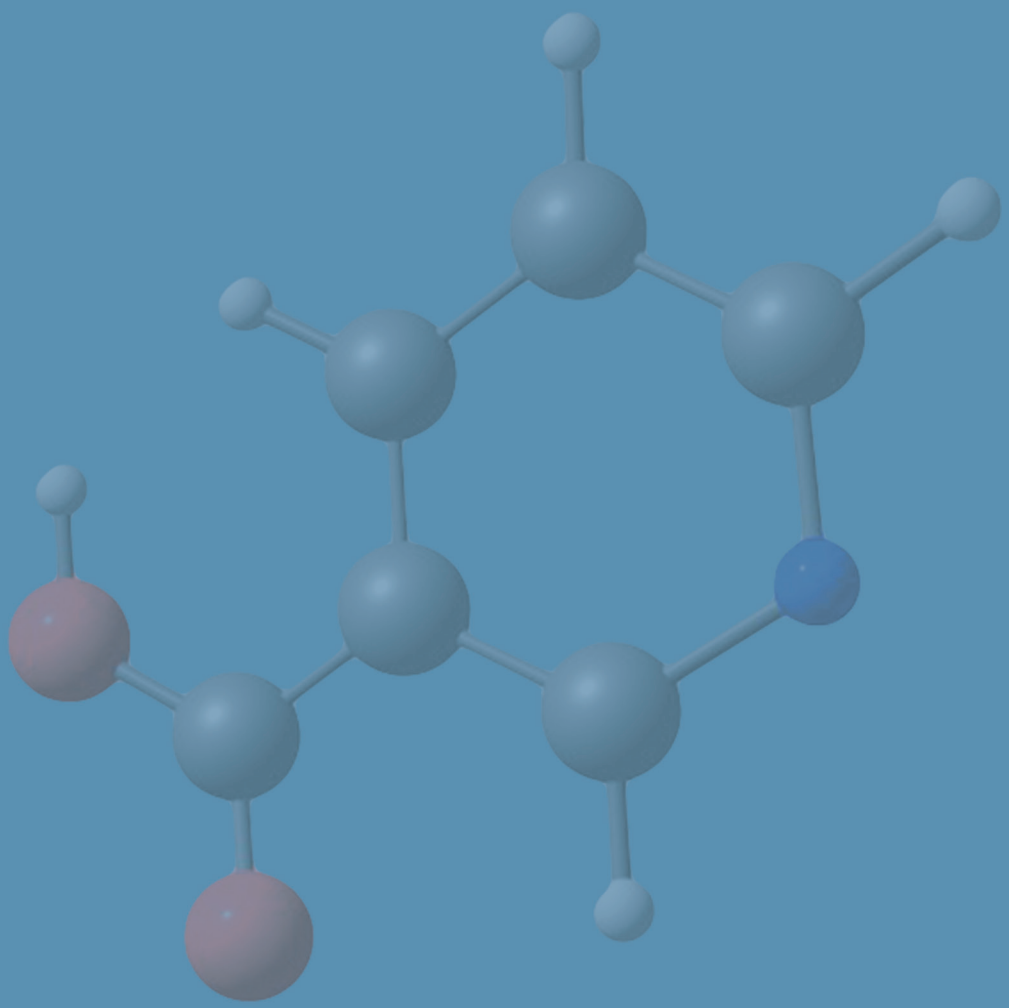

BILINGUAL
PUBLISHING CO.
Pioneer of Global Academics Since 1984

Tel:+65 65881289
E-mail: contact@bilpublishing.com
Website:ojs.bilpublishing.com

ISSN 2661-3875
01